Real space topology for moiré materials

Christophe Mora

Laboratoire Matériaux et Phénomènes Quantiques

Outline

I. Chern and fractional Chern insulators in 2D materials

II. Layer skyrmion in adiabatic twisted TMD and chiral TBG

III. Real-space topology and ensembles of Bloch wavefunctions

Chern and fractional Chern insulators in 2D materials

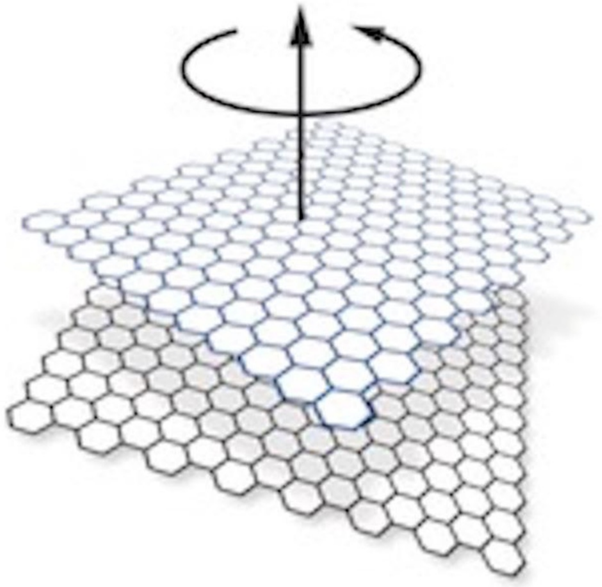

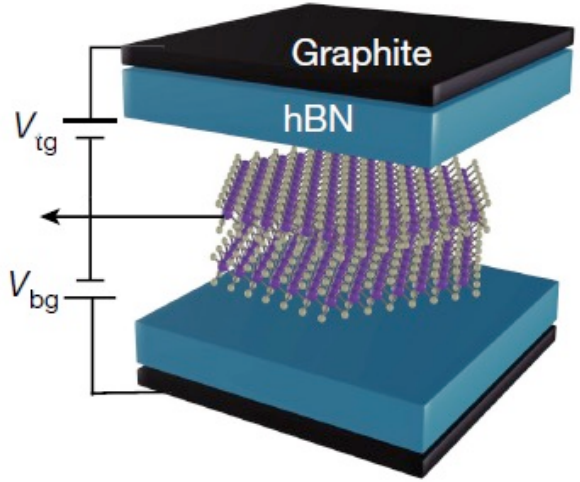

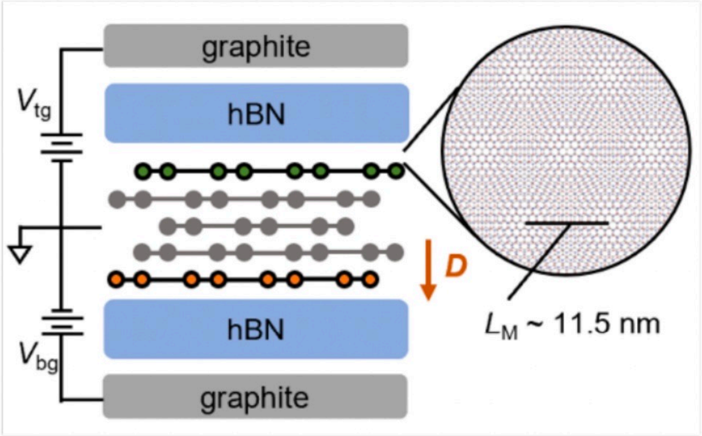

Science *Science* **360**, 62-66. (2018) REPORTS

Observation of fractional Chern insulators in a van der Waals heterostructure

Eric M. Spanton,[1]* Alexander A. Zibrov,[2]* Haoxin Zhou,[2] Takashi Taniguchi,[3] Kenji Watanabe,[3] Michael P. Zaletel,[4] Andrea F. Young[2]†

[1]California Nanosystems Institute, University of California, Santa Barbara, CA 93106, USA. [2]Department of Physics, University of California, Santa Barbara, CA 93106, USA. [3]Advanced Materials Laboratory, National Institute for Materials Science, Tsukuba, Ibaraki 305-0044, Japan. [4]Department of Physics, Princeton University, Princeton, NJ 08544, USA.

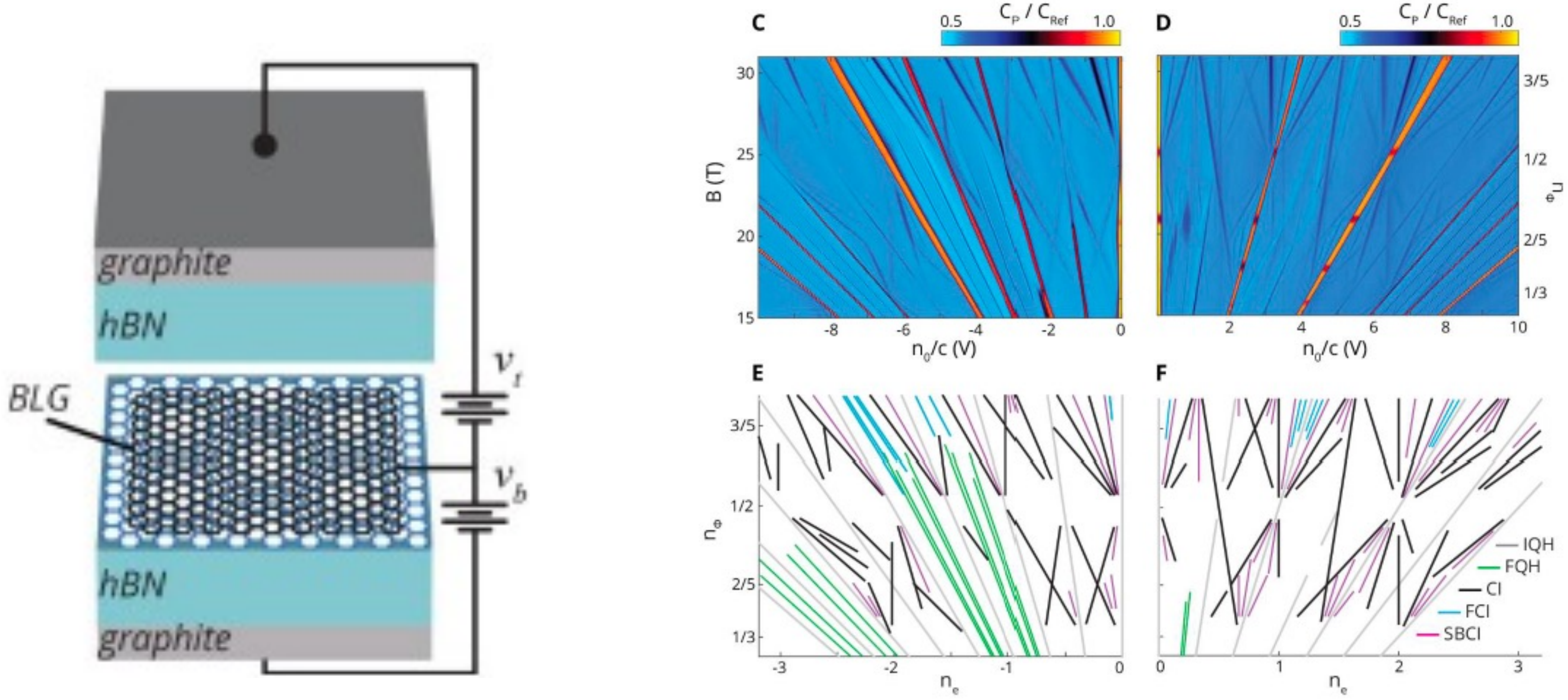

Narrow bands in 2D materials

TBG $\theta = 1.05^o$

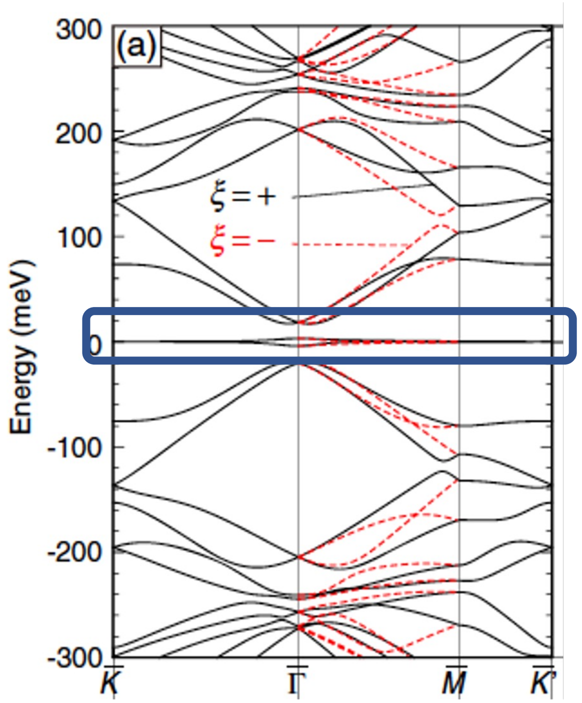

Koshino et al., PRX 2018

Moiré pattern

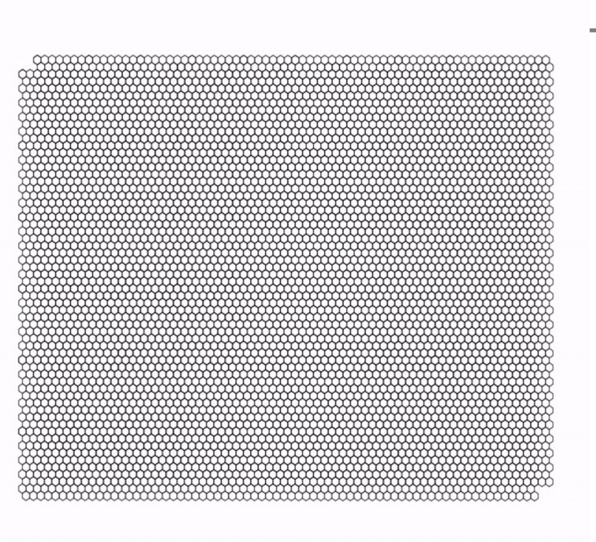

tMoTe$_2$

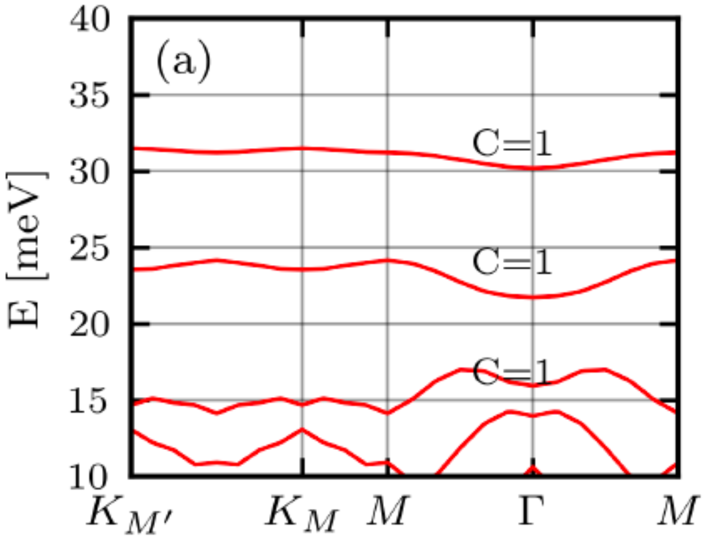

Zhang, Wang, Liu, Fan, Cao, and Xiao, Nature Comm 2024

Rhombo. Pentalayer Graphene

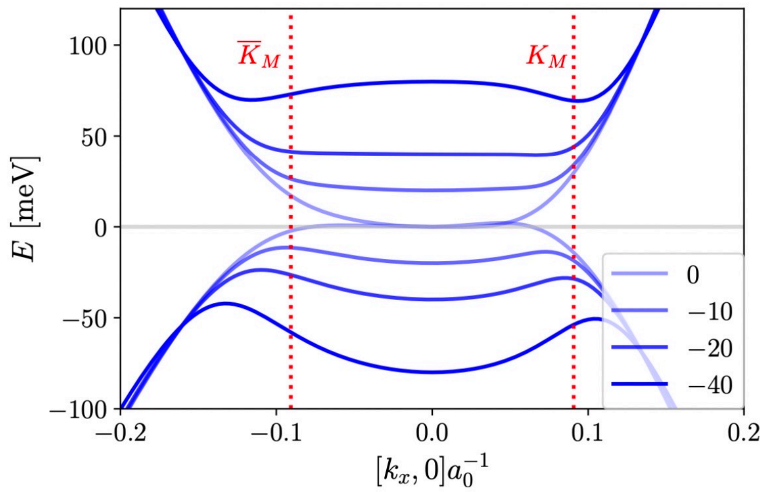

Ferromagnetic states and Chern insulators

Zondiner, Ilani, Nature 2020 ; Wong, Yazdani, Nature 2020 ; Saito, Young, Nature Physics 2021

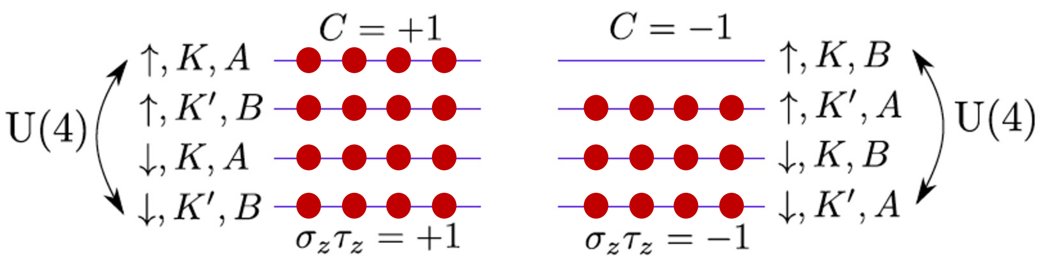

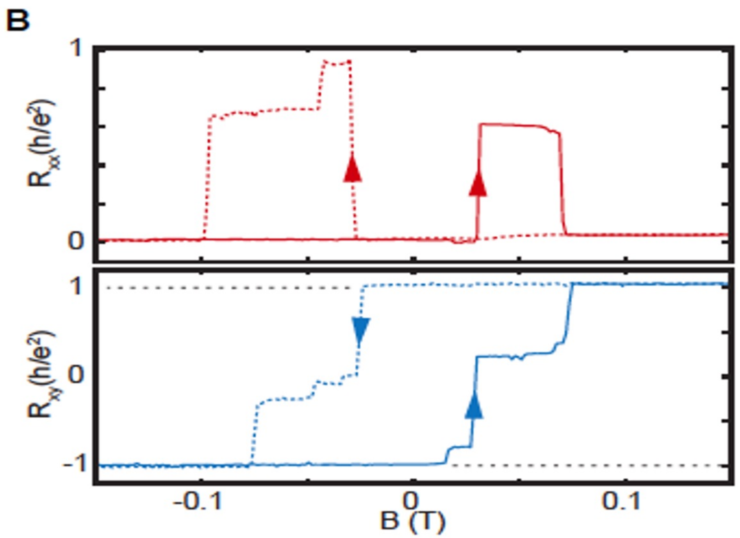

Serlin, Tschirhart, Balents, Young, et al. Science 2020

Sharpe, Golhaber-Gordon, et al. Science 2019

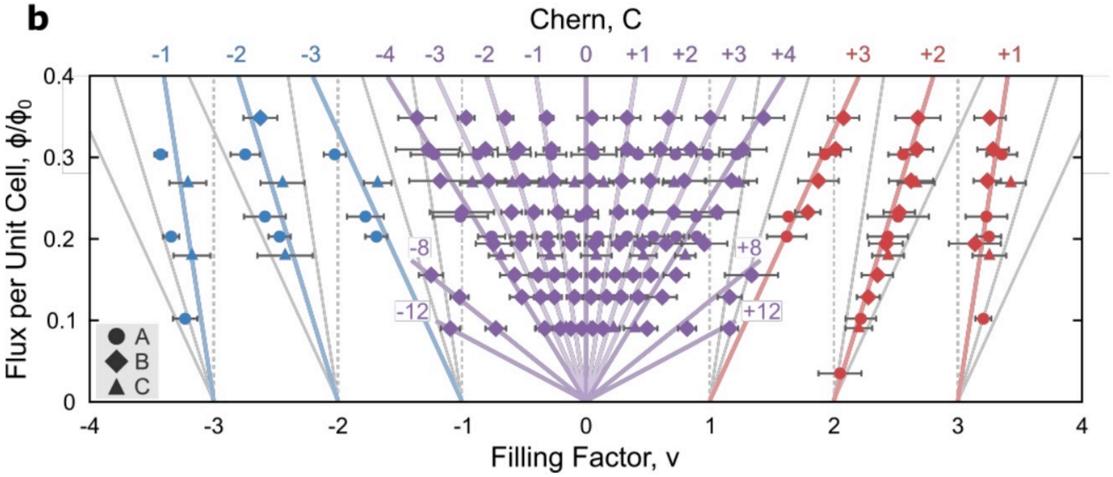

Nuckolls, Wong, …, Bernevig, Yazdani Nature 2020

Wang, Vafek PRX 2024

Fractional Chern insulators in TBG

TBG

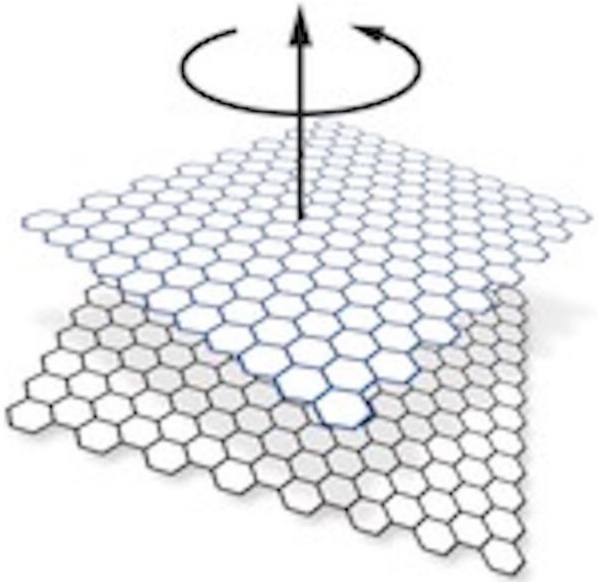

Xie, Jarillo-Herrero, Yacoby, Nature 2021

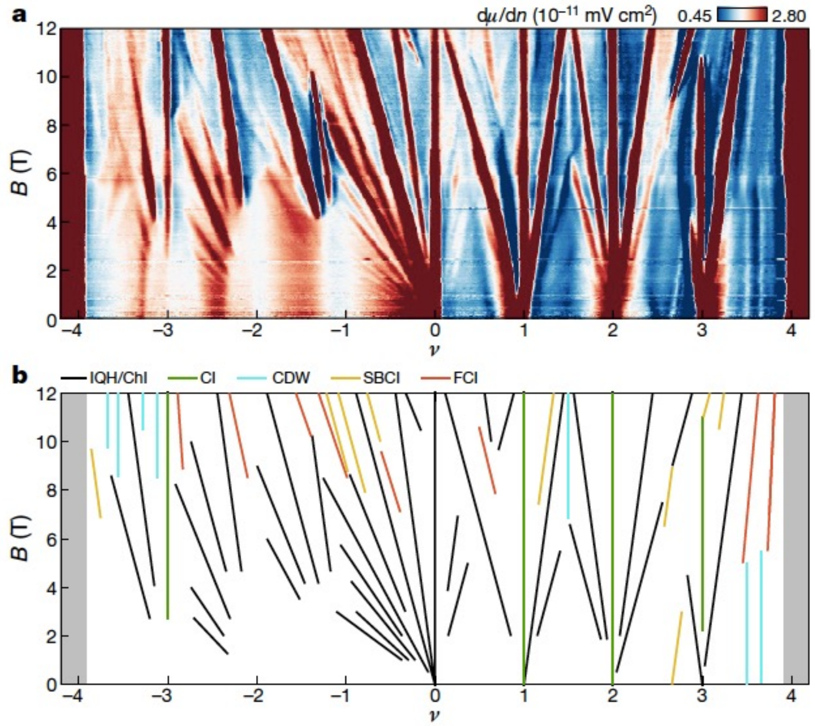

Fractional Chern insulators identified in Fan diagrams

They are stabilized above 5T

Fractional Chern insulators

$tMoTe_2$ $\theta = 3.7°$

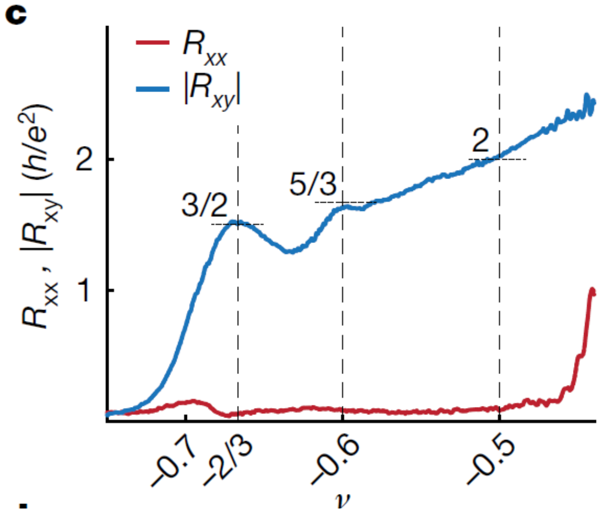

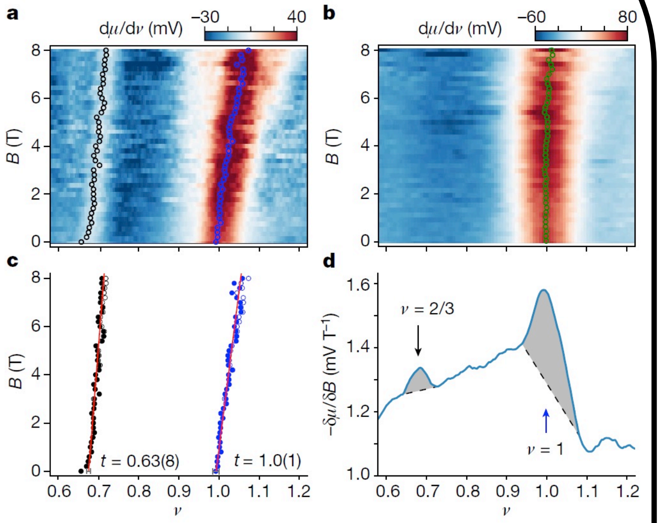

Cai, Anderson, Wang, Zhang, Liu, Holtzmann, Zhang, Fan, Taniguchi, Watanabe, Ran, Cao, Fu, Xiao, Yao, and Xu, Nature 2023

Zeng, Xia, Kang, Zhu, Knüppel, Vaswani, Watanabe, Taniguchi, Mak, and Shan, 2023. Nature 622, 69–73.

Park, Cai, Anderson, Zhang, Zhu, Liu, Wang, Holtzmann, Hu, Liu, Taniguchi, Watanabe, Chu, Cao, Fu, Yao, Chang, Cobden, Xiao, and Xu, 2023. Nature 622, 74–79.

Kang, Shen, Qiu, Zeng, Xia, Watanabe, Taniguchi, Shan, and Mak, 2024. Nature 628, 522–526.

Rhombo. Pentalayer Graphene

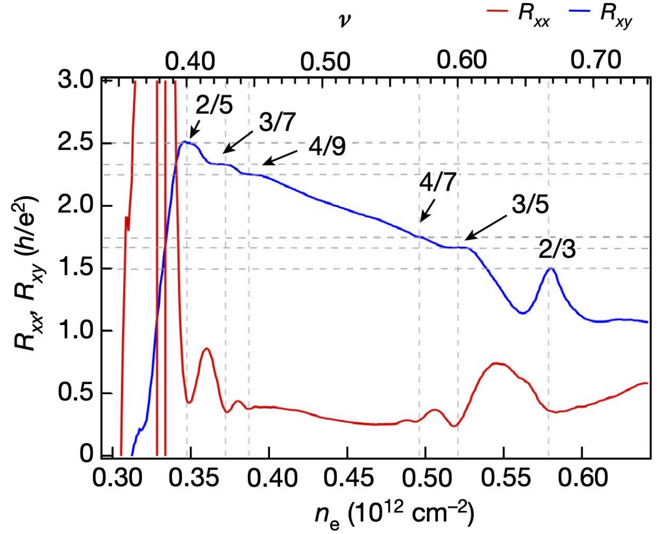

Lu, Han, Yao, Reddy, Yang, Seo, Watanabe, Taniguchi, Fu and Long, Nature 2023

FCIs in TMDs

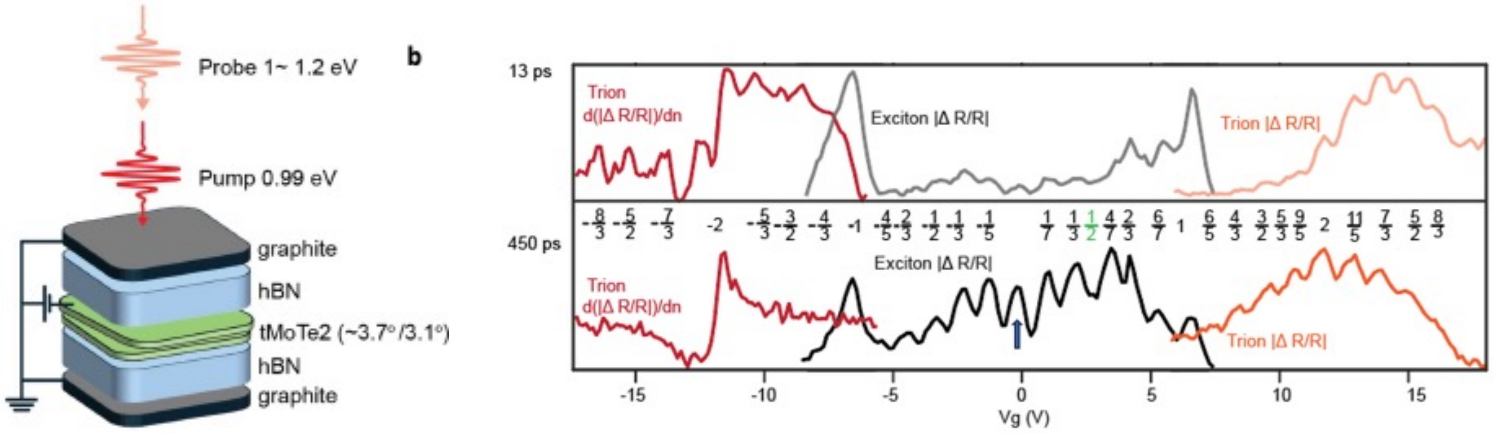

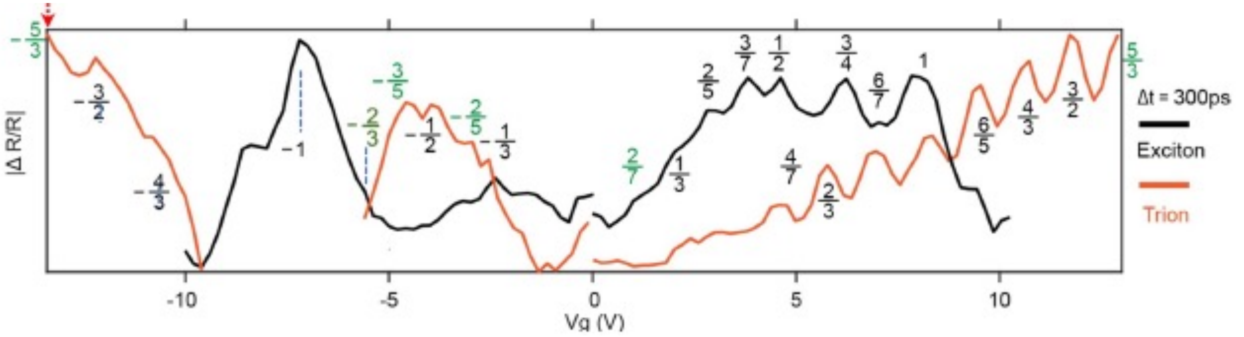

Yiping Wang, Jeongheon Choe, Eric Anderson, Weijie Li, Julian Ingham, Eric A. Arsenault, Yiliu Li, Xiaodong Hu, Takashi Taniguchi, Kenji Watanabe, Xavier Roy, Dmitri Basov, Di Xiao, Raquel Queiroz, James C. Hone, Xiaodong Xu, X.-Y. Zhu, arXiv:2502.21153

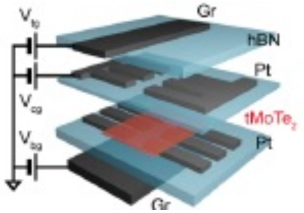

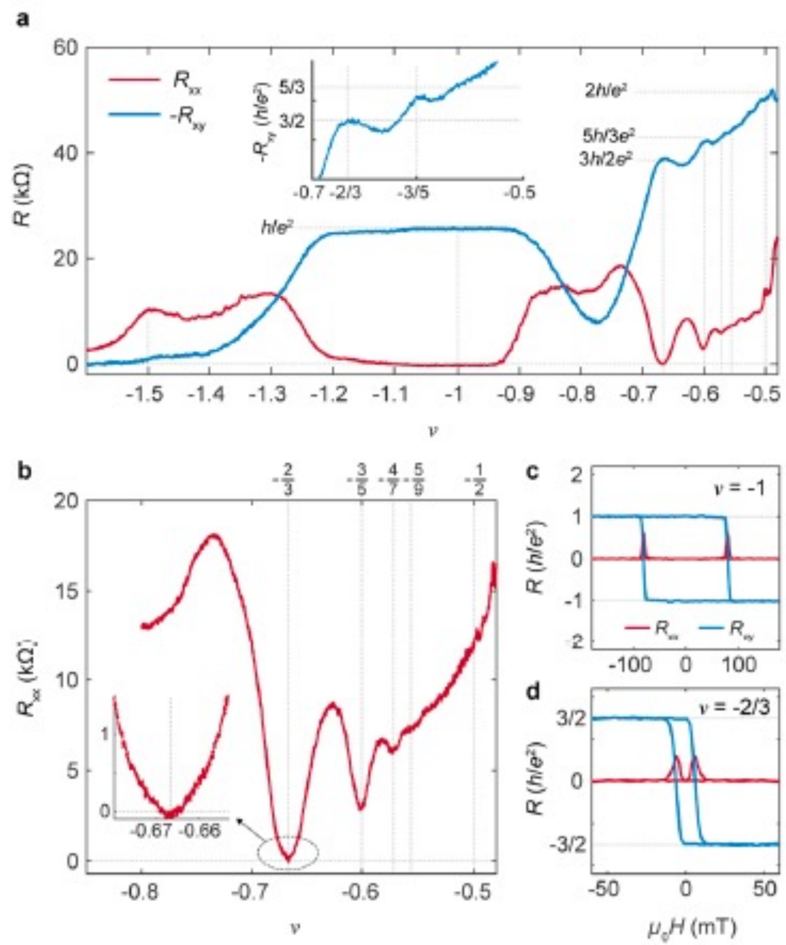

FCIs in rhombohedral graphene

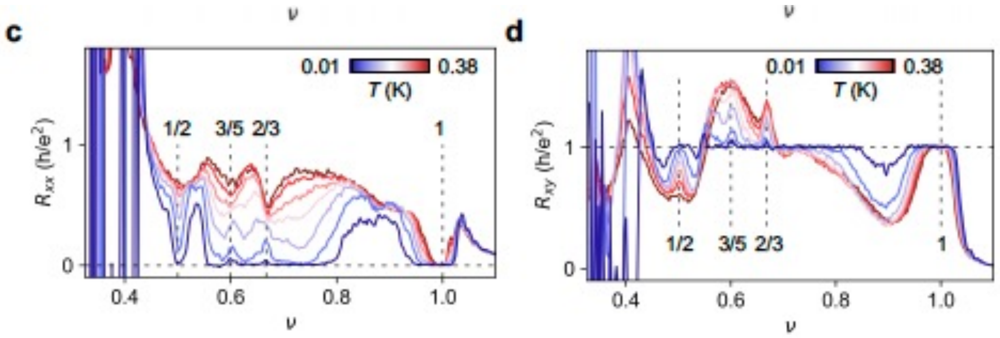

Z. Lu, T. Han, Y. Yao, Z. Hadjri, J. Yang, J. Seo, L. Shi, S. Ye, K. Watanabe, T. Taniguchi, and L. Ju, **Nature** 637, 1090 (2025).

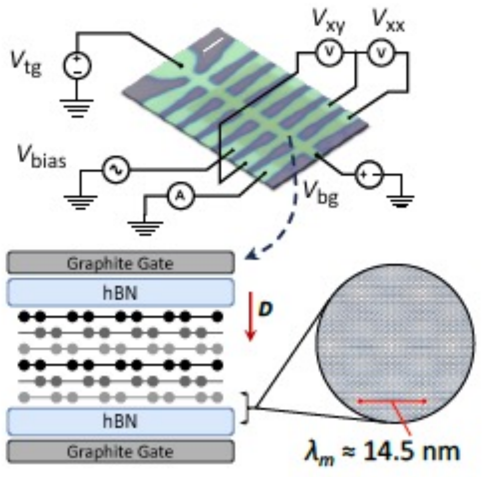

Hexalayer

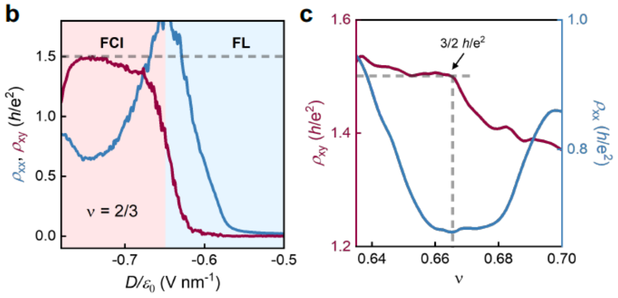

Xie, Huo, Lu, Feng, Zhang, Wang, Yang, Watanabe, Taniguchi, Liu, Song, Xie, Liu & Lu. **Nature Materials** (2025).

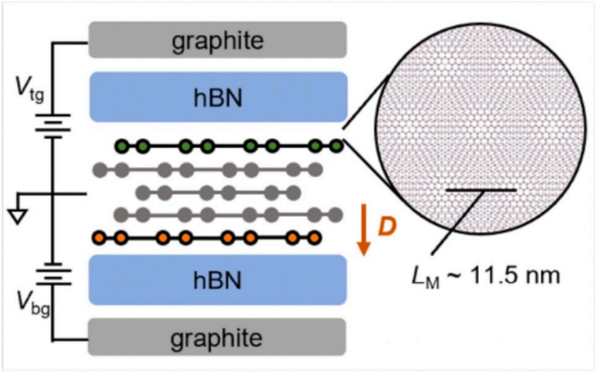

Tetralayer

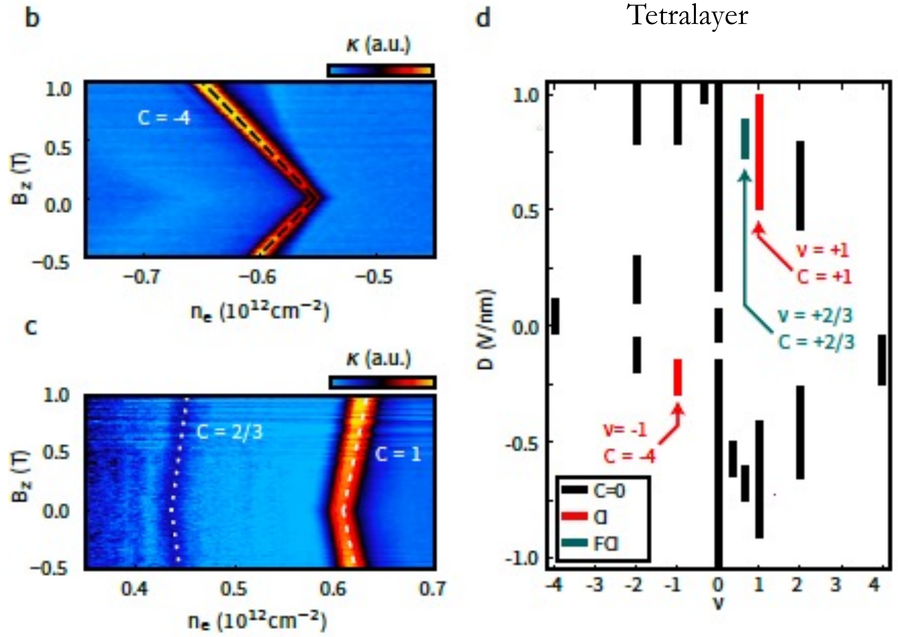

Choi, Y., Choi, Y., Valentini, M., Patterson, C. L., Holleis, L. F. W., Sheekey, O. I., Stoyanov, H., Cheng, X., Taniguchi, T., Watanabe, K. & Young, A. F., **Nature**, 639, 342–347 (2025).

Layer skyrmion in adiabatic TMD and chiral TBG

Layer skyrmions for ideal Chern bands and twisted bilayer graphene

Daniele Guerci,[1] Jie Wang,[2] and Christophe Mora[3]

[1] *Center for Computational Quantum Physics, Flatiron Institute, New York, New York 10010, USA*
[2] *Department of Physics, Temple University, Philadelphia, Pennsylvania, 19122, USA*
[3] *Université Paris Cité, CNRS, Laboratoire Matériaux et Phénomènes Quantiques, 75013 Paris, France*

arXiv:2408.12652v1

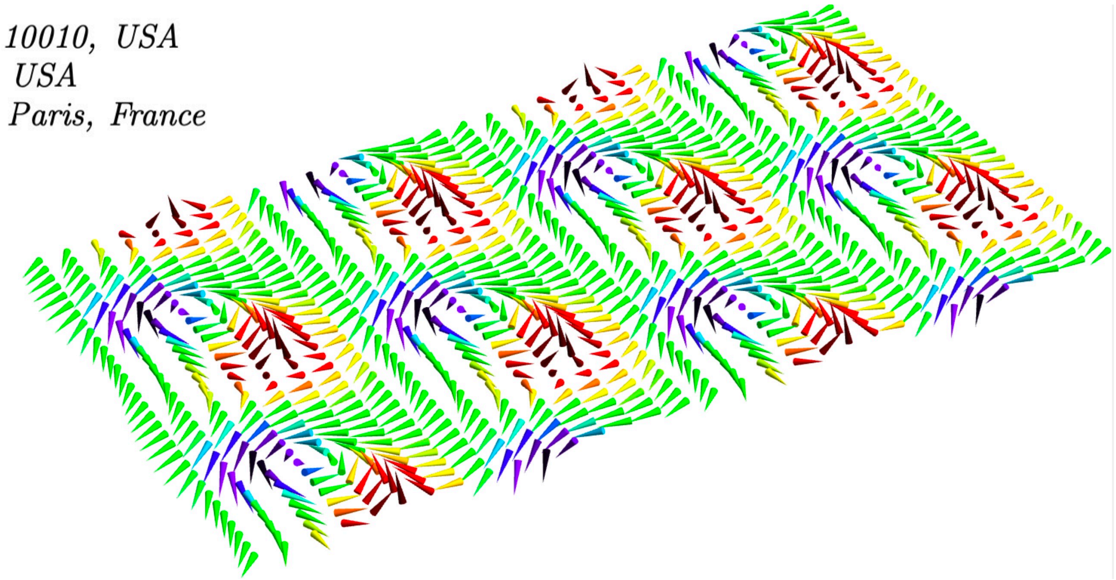

Continuum model for twisted TMD - WSe_2 $MoTe_2$

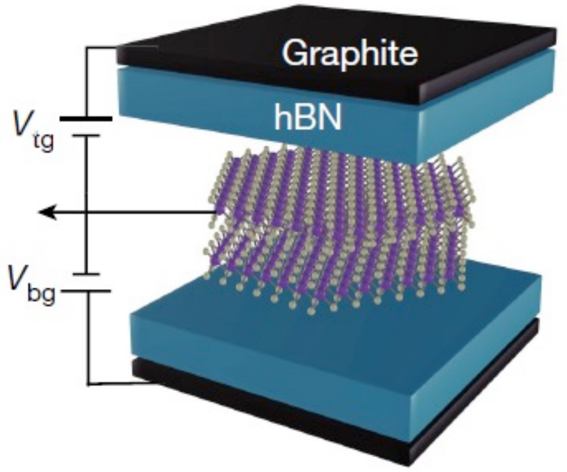

$$H_{\rm sp}^K = \begin{pmatrix} -\frac{\hbar^2(\mathbf{k}-\mathbf{K}^b)^2}{2m^*} + V_b(\mathbf{r}) & T(\mathbf{r}) \\ T^\dagger(\mathbf{r}) & -\frac{\hbar^2(\mathbf{k}-\mathbf{K}^t)^2}{2m^*} + V_t(\mathbf{r}) \end{pmatrix}$$

$$T(\mathbf{r}) = w(1 + e^{-i\mathbf{g}_2\cdot\mathbf{r}} + e^{-i\mathbf{g}_3\cdot\mathbf{r}})$$

Parameters chosen to fit ab initio DFT calculations

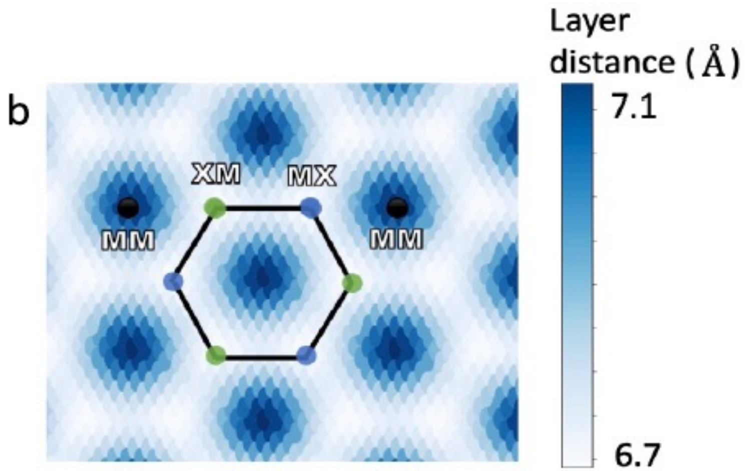

Wu, Lovorn, Tutuc, Martin, MacDonald PRL 2019

$$H_{sp}^K = -\frac{(\hbar\mathbf{k})^2}{2m^*}\sigma_0 + \mathbf{\Delta}(\mathbf{r})\cdot\boldsymbol{\sigma} + \Delta_0(\mathbf{r})\sigma_0,$$

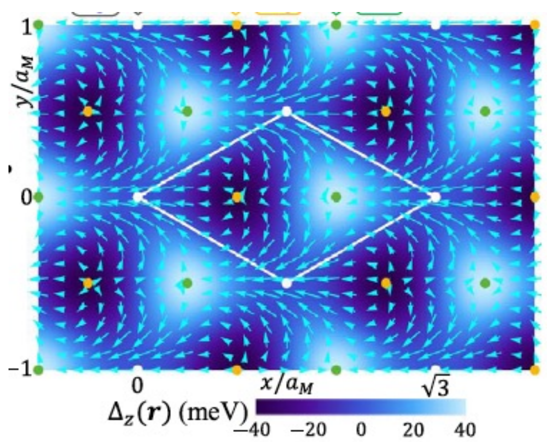

Pontryagin index/unit cell $= 1$

Adiabatic approximation

Morales-Durán, Wei, Shi, and MacDonald, 2024. Phys. Rev. Lett. 132, 096602.

Zhai and Yao, 2020. Phys. Rev. Mater. 4, 094002.

Bruno, Dugaev, and Taillefumier, 2004. Phys. Rev. Lett. 93, 096806.

$$H_{sp}^{K} = -\frac{(\hbar \mathbf{k})^2}{2m^*}\sigma_0 + \boldsymbol{\Delta}(\mathbf{r})\cdot\boldsymbol{\sigma} + \Delta_0(\mathbf{r})\sigma_0,$$

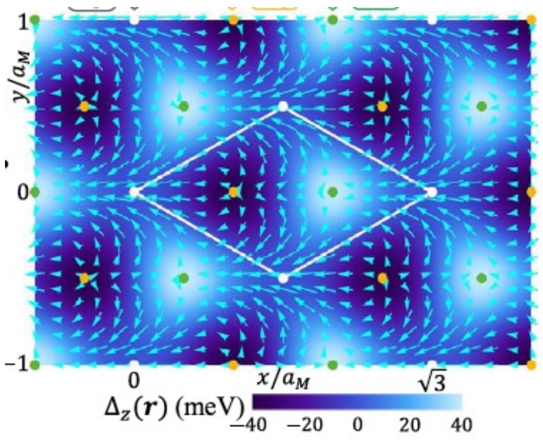

Similar to Born-Oppenheimer $\quad \psi_{\boldsymbol{k}}(\boldsymbol{r}) = \boldsymbol{\chi}(\boldsymbol{r})\,\Phi_{\boldsymbol{k}}(\boldsymbol{r})$

Spinor follows the vector $\boldsymbol{\Delta}(\mathbf{r})$

Scalar function

The scalar part experiences a fictitious magnetic field

$$\left\{-\frac{(-i\hbar\nabla - e\tilde{\mathbf{A}}(\mathbf{r}))^2}{2m^*} + \tilde{V}(\mathbf{r})\right\}\Phi_k(\mathbf{r}) = \varepsilon_k \Phi_k(\mathbf{r})$$

$$\hat{\boldsymbol{n}}(\mathbf{r}) = \frac{\boldsymbol{\Delta}(\mathbf{r})}{|\boldsymbol{\Delta}(\mathbf{r})|} \qquad \tilde{B}(\mathbf{r}) = -\frac{\hbar}{2e}\hat{\mathbf{n}}(\mathbf{r})\cdot\partial_x\hat{\mathbf{n}}(\mathbf{r})\times\partial_y\hat{\mathbf{n}}(\mathbf{r})$$

One flux quantum per unit cell

The geometric phase of the winding acts as the Aharonov-Bohm phase of the fictitious magnetic field

Hofstadter spectra for TMDs

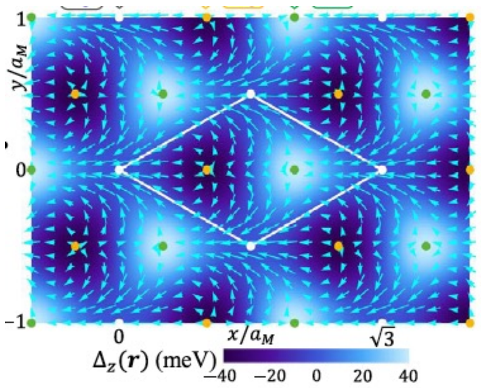

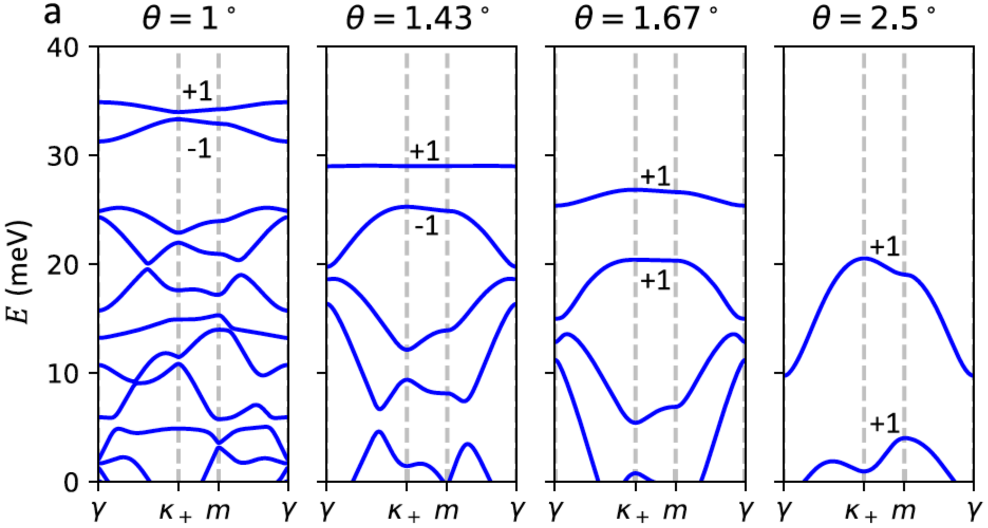

WSe$_2$

Devakul, Crepel, Zhang, Fu Nat Comm 2021

WSe$_2$ $\theta = 1.67^\circ$

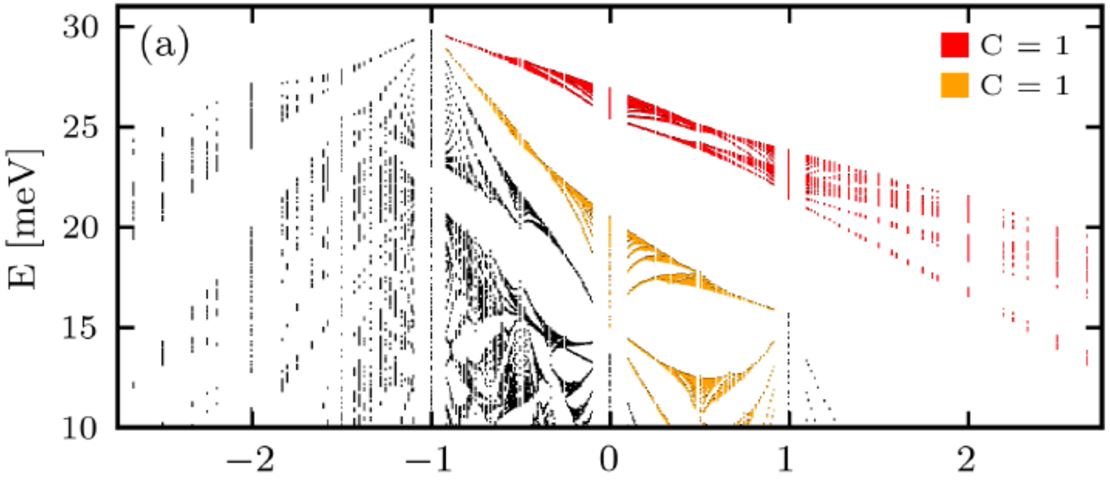

MoTe$_2$ $\theta = 2.1^\circ$

Kolar, K. Wang, von Oppen, Mora PRB 2024

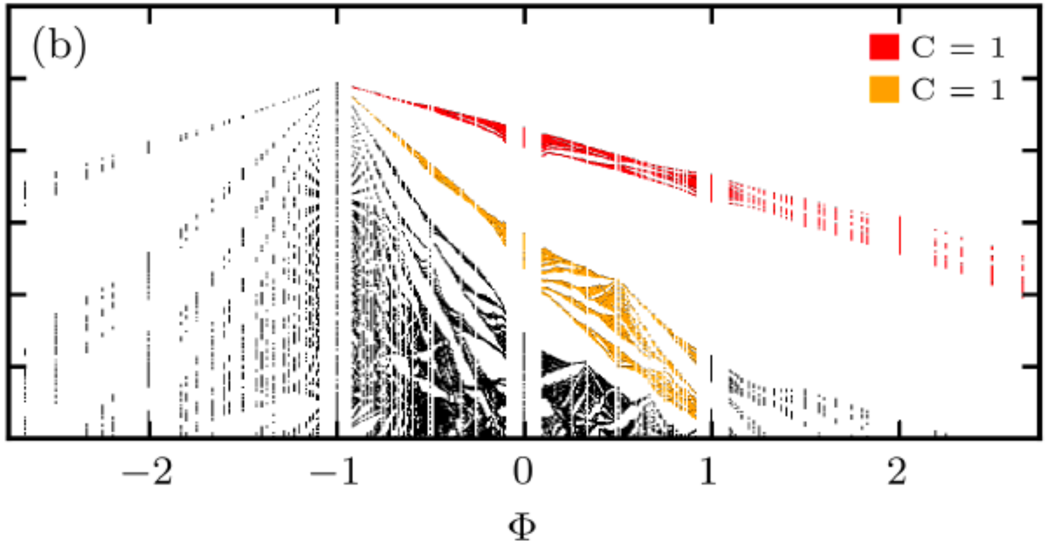

Wavefunction zeros in the adiabatic approximation

$$\left\{-\frac{(-i\hbar\nabla - e\tilde{\mathbf{A}}(\mathbf{r}))^2}{2m^*} + \tilde{V}(\mathbf{r})\right\}\Phi_k(\mathbf{r}) = \varepsilon_k \Phi_k(\mathbf{r})$$

$$\psi_{\boldsymbol{k}}(\boldsymbol{r}) = \boldsymbol{\chi}(\boldsymbol{r})\,\Phi_{\boldsymbol{k}}(\boldsymbol{r})$$

The Aharonov-Bohm phase imposes one zero and an associated vortex for each unit cell (Riemann-Roch theorem)

These zeros are perturbatively not stable. They are lifted by deviations from the adiabatic limit

A real-space Berry connection can be defined

$$A(\mathbf{r}) = -i\chi^\dagger(\mathbf{r})\nabla_{\mathbf{r}}\chi(\mathbf{r})$$

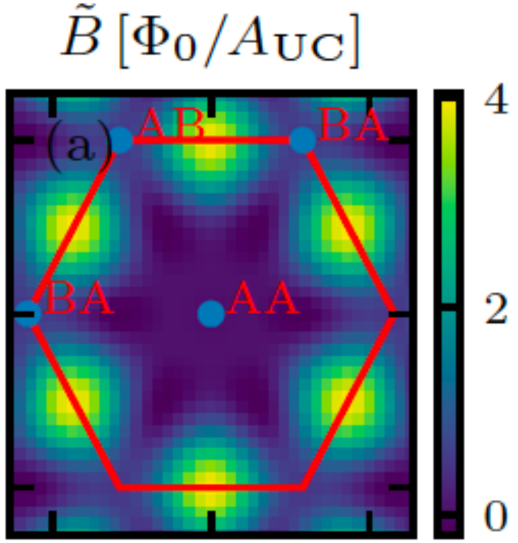

The real-space Berry curvature integrates to -1.

Twisted bilayer graphene – chiral limit

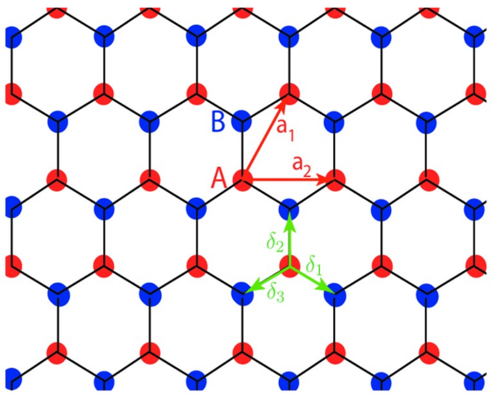

Chiral limit: vanishing AA (BB) hoppings

$$H = \begin{pmatrix} 0 & \mathcal{D}^\dagger \\ \mathcal{D} & 0 \end{pmatrix} \qquad \mathcal{D} = -i\partial_{\bar z} + \begin{pmatrix} 0 & f_2(\boldsymbol{r}) \\ f_1^*(\boldsymbol{r}) & 0 \end{pmatrix}$$

Zero-energy solution is also a zero mode of $\mathcal{D}$

$$\begin{cases} \mathcal{D}\,\psi_K(\boldsymbol{r}) = 0 \\ \psi_{\mathbf{k}}(\boldsymbol{r}) = g(z)\psi_K(\boldsymbol{r}) \end{cases} \Longrightarrow \quad \mathcal{D}\,\psi_k(\boldsymbol{r}) = 0$$

g(z) is an arbitrary holomorphic function of z

Same structure as the lowest Landau level (vortexability)

Landau level correspondence for chiral TBG

At the magic angle (and chiral limit), decomposition of the WF into scalar LLL and a spinor

$$\psi_{\boldsymbol{k}}(\boldsymbol{r}) = \boldsymbol{\chi}(\boldsymbol{r})\, \Phi_{\boldsymbol{k}}^{LLL}(\boldsymbol{r})$$

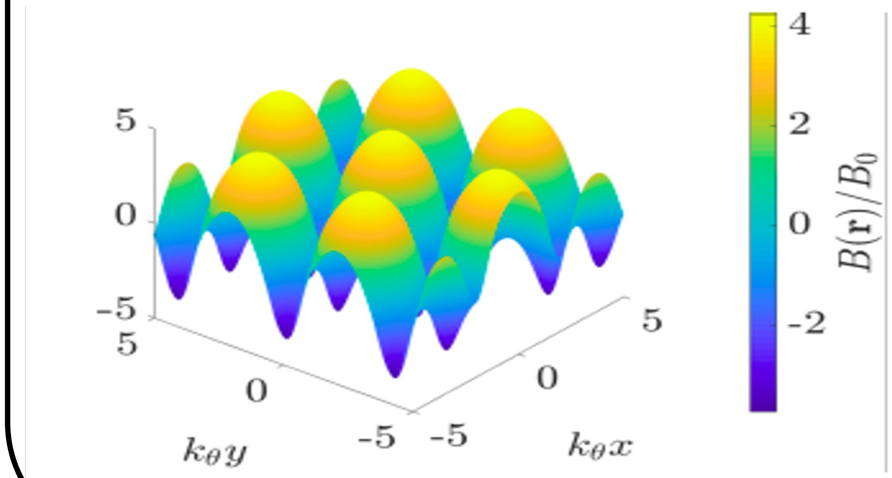

$$\chi(\boldsymbol{r}) = \begin{pmatrix} \chi_1(\boldsymbol{r}) \\ \chi_2(\boldsymbol{r}) \end{pmatrix}$$

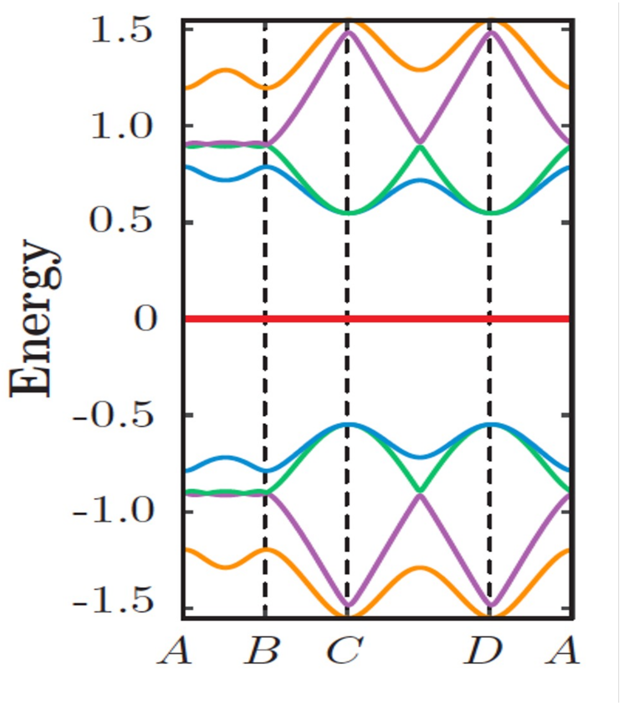

Again, one zero in the LLL WF per unit cell

Skyrmion texture in real space for chiral TBG

Guerci, Wang, Mora Arxiv 2024

$$\psi_{\boldsymbol{k}}(\boldsymbol{r}) = \boldsymbol{\chi}(\boldsymbol{r})\,\Phi_{\boldsymbol{k}}^{LLL}(\boldsymbol{r}) \qquad \chi(\boldsymbol{r}) = \begin{pmatrix} \chi_1(\boldsymbol{r}) \\ \chi_2(\boldsymbol{r}) \end{pmatrix} \qquad A(\mathbf{r}) = -i\chi^\dagger(\mathbf{r})\nabla_{\mathbf{r}}\chi(\mathbf{r})$$

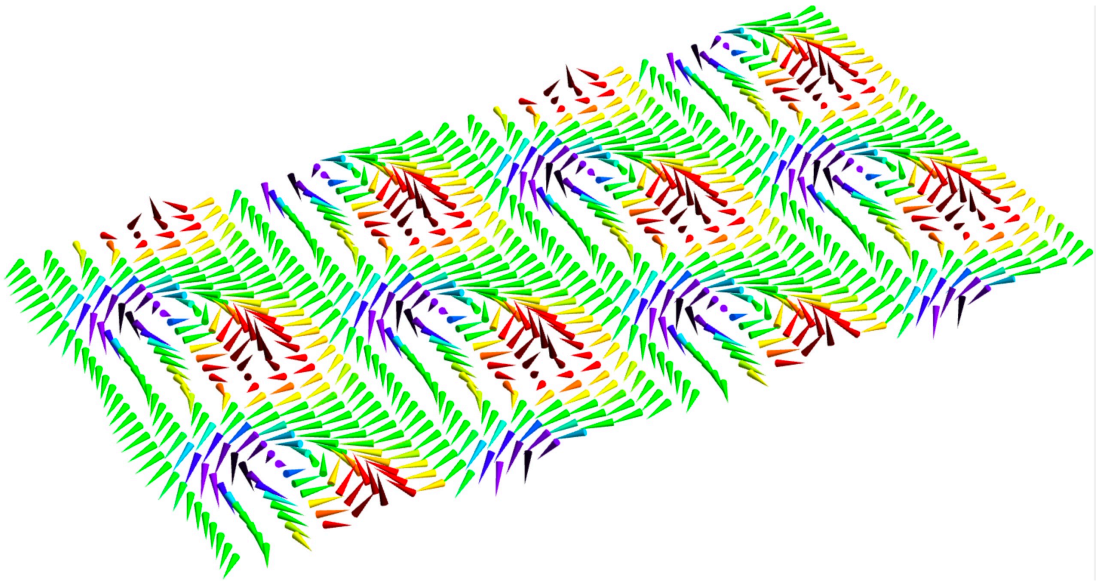

Layer skyrmion texture for a Chern C=1 band

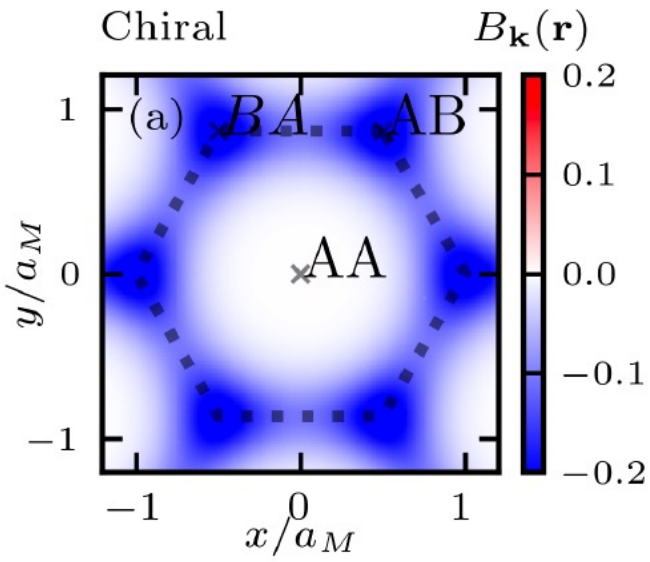

Real-space Chern number =

Pontryagin index = -1

Summary: adiabatic twisted TMD and chiral TBG

LL – spinor decomposition $\psi_{\boldsymbol{k}}(\boldsymbol{r}) = \chi(\boldsymbol{r})\,\Phi_{\boldsymbol{k}}(\boldsymbol{r})$

Scalar part experiences an effective magnetic field with a flux quantum through the unit cell

One zero per unit cell, unstable against perturbation

Skyrmion texture for the spinor. Real-space Chern number or Pontryagin index of -1

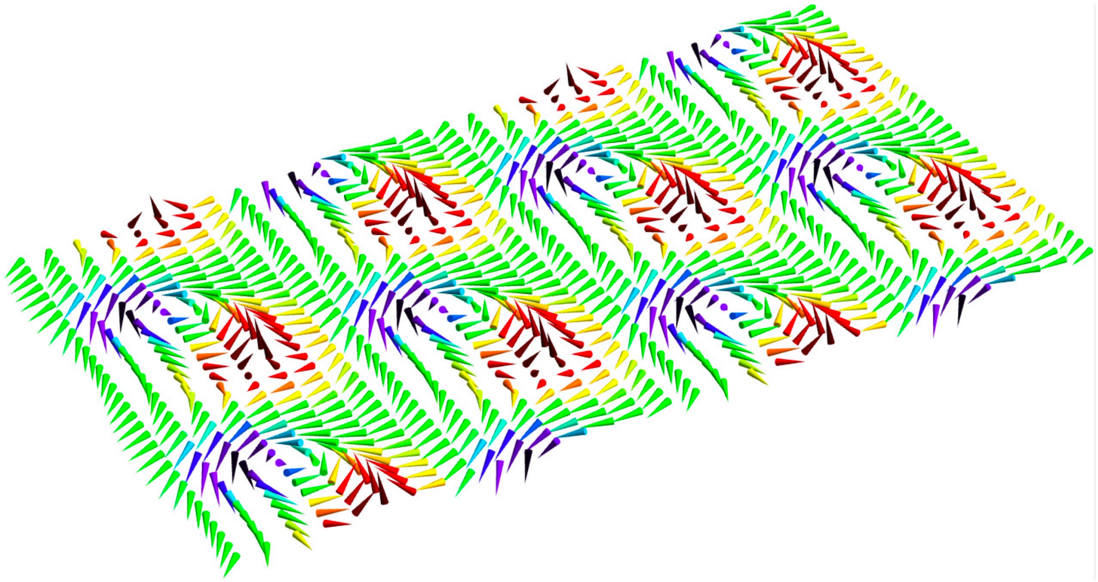

Real-space topology and ensemble of Bloch wavefunctions

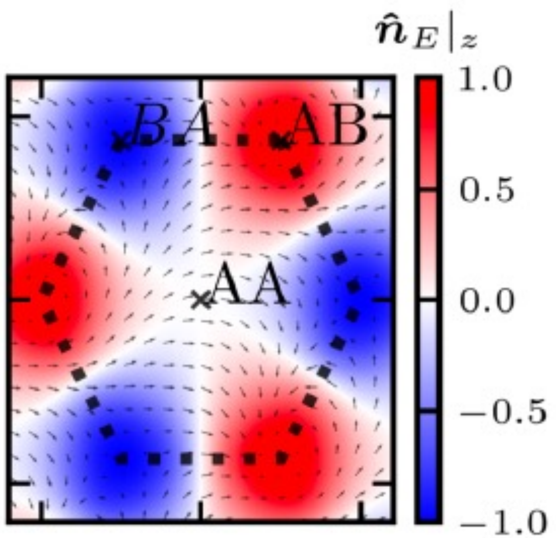

Beyond the ideal cases (TMDs or TBG)

Mathematical theorem. If $\psi_{\boldsymbol{k}}(\boldsymbol{r})$ is never vanishing and periodic over the lattice : the real-space Chern number is always zero.

$$u_{\mathbf{k}}(\mathbf{r}) = \chi(\mathbf{r})\Phi_{\mathbf{k}}(\mathbf{r}) + \epsilon\Delta u_{\mathbf{k}}(\mathbf{r})$$

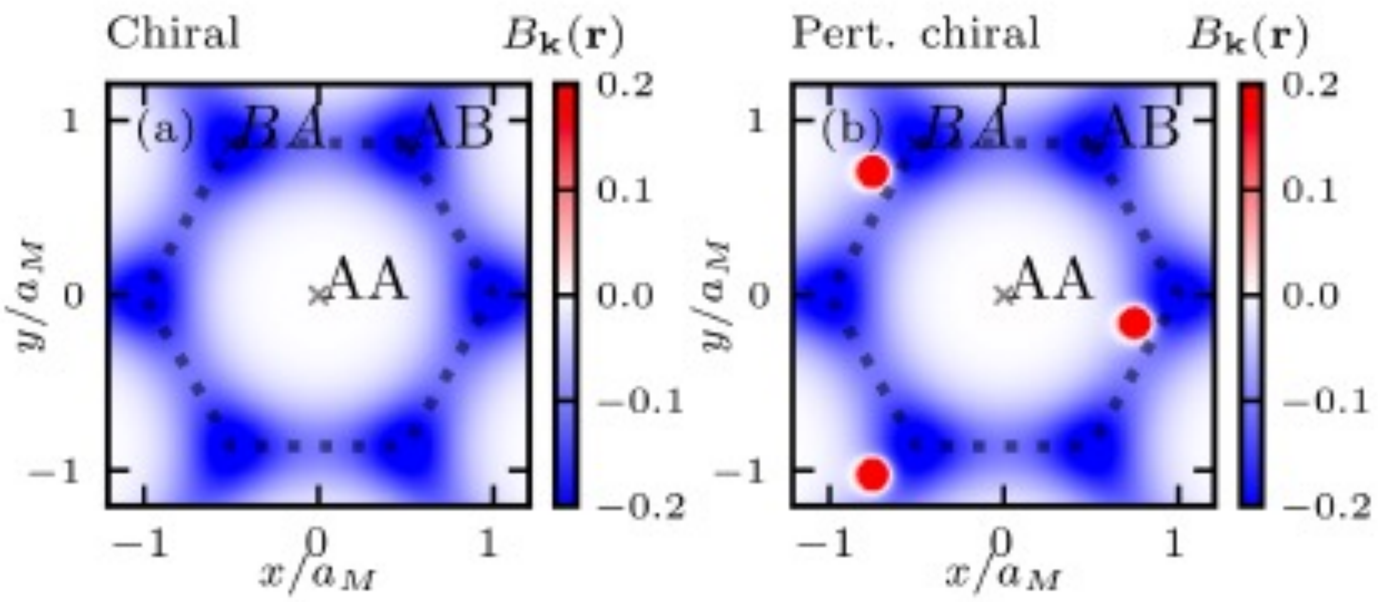

Example in TBG at angle with realistic corrugation

Lifting of the zero (perturbation) : small region with strong positive contribution to the real-space Chern number.

Compensate the negative part.

Real-space skyrmion for TMD

$$u_{\mathbf{k}}(\mathbf{r}) = \chi(\mathbf{r})\Phi_{\mathbf{k}}(\mathbf{r}) + \epsilon\Delta u_{\mathbf{k}}(\mathbf{r})$$

Non-adiabatic limit

$$\hat{\boldsymbol{n}}_{\mathbf{k}}(\mathbf{r}) = \frac{u^\dagger_{\mathbf{k}}(\mathbf{r})\boldsymbol{\sigma} u_{\mathbf{k}}(\mathbf{r})}{u^\dagger_{\mathbf{k}}(\mathbf{r}) u_{\mathbf{k}}(\mathbf{r})}$$

Reduces to (in the adiabatic limit)

$$\hat{\boldsymbol{n}}(\mathbf{r}) = \chi^\dagger(\mathbf{r})\boldsymbol{\sigma}\chi\ (\mathbf{r})$$

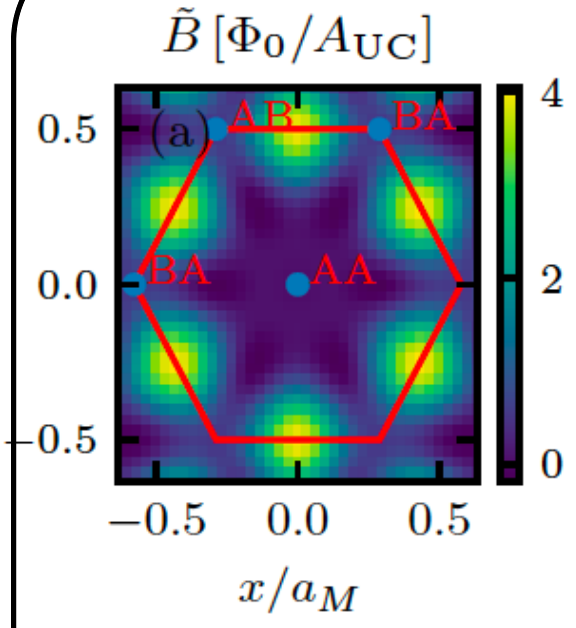

Adiabatic limit

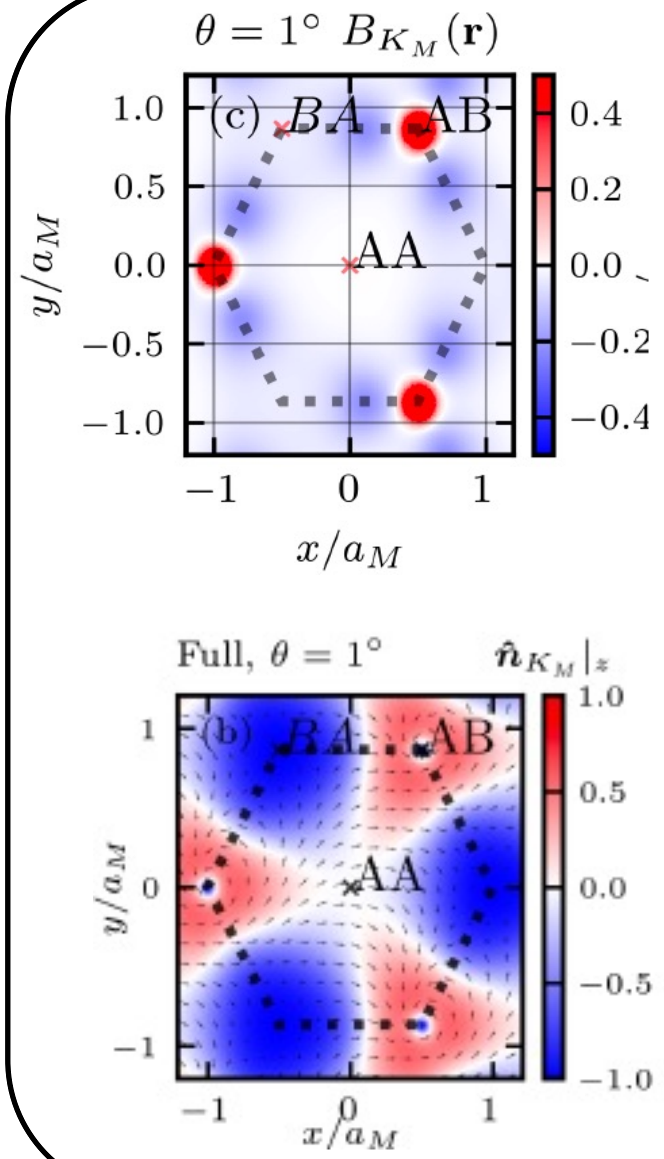

Real-space topology – individual vs ensemble of WFs

So far, we explored individual (at fixed momentum) WF

$$u_{\mathbf{k}}(\mathbf{r}) = \chi(\mathbf{r})\Phi_{\mathbf{k}}(\mathbf{r}) + \epsilon\Delta u_{\mathbf{k}}(\mathbf{r})$$

Generally, they have zero real-space Chern number, despite exhibing (close to) skyrmion textures

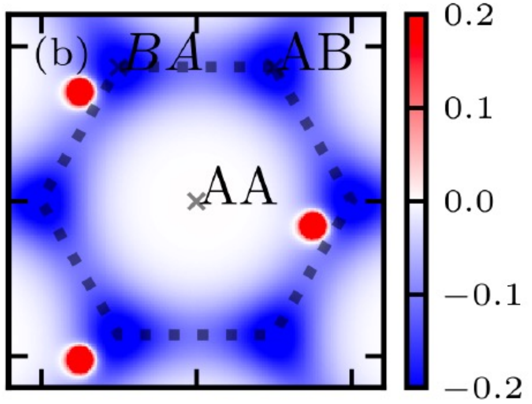

We introduce an ensemble average – similar to tunneling density of states

$$\boldsymbol{A}(E,\mathbf{r}) = \sum_{\mathbf{k}} u^{\dagger}_{\mathbf{k}}(\mathbf{r})\boldsymbol{\sigma} u_{\mathbf{k}}(\mathbf{r})\delta(\epsilon_{\mathbf{k}} - E)$$

$$\hat{\boldsymbol{n}}_E(\mathbf{r}) = \frac{\boldsymbol{A}(E,\mathbf{r})}{|\boldsymbol{A}(E,\mathbf{r})|}$$

Non-trivial spatial winding of this vector (Pontryagin index)

Ensemble of WFs - TMDs

Adiabatic vs individual WF vs ensemble

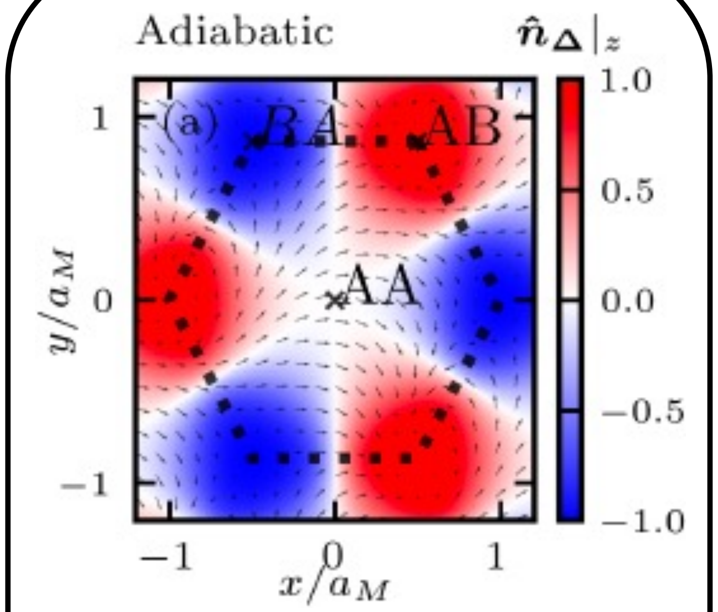

Adiabatic spinor WF

$$C_R = -1$$

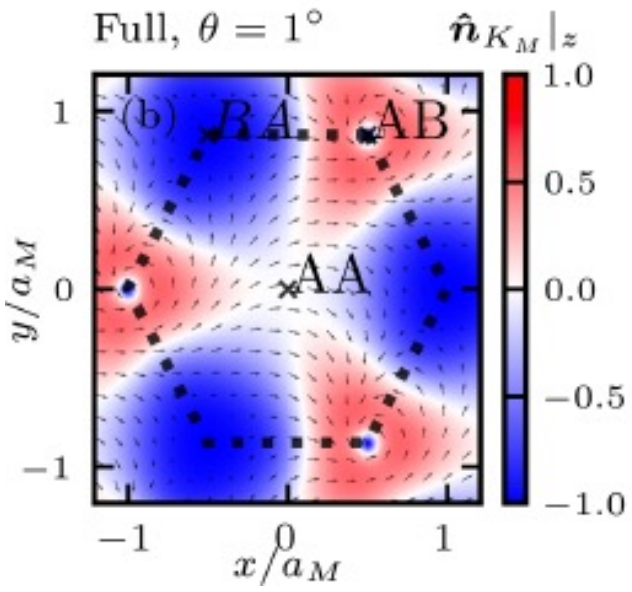

WF at momentum k

$$C_R = 0$$

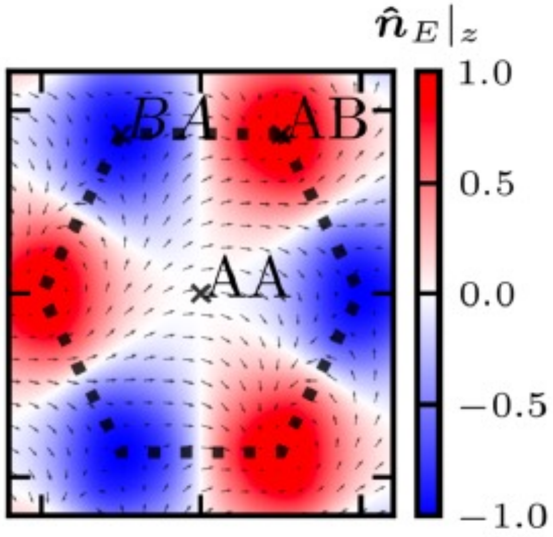

Ensemble of WF

(fixed energy)

$$C_R = -1$$

Real-space Chern number from ensemble

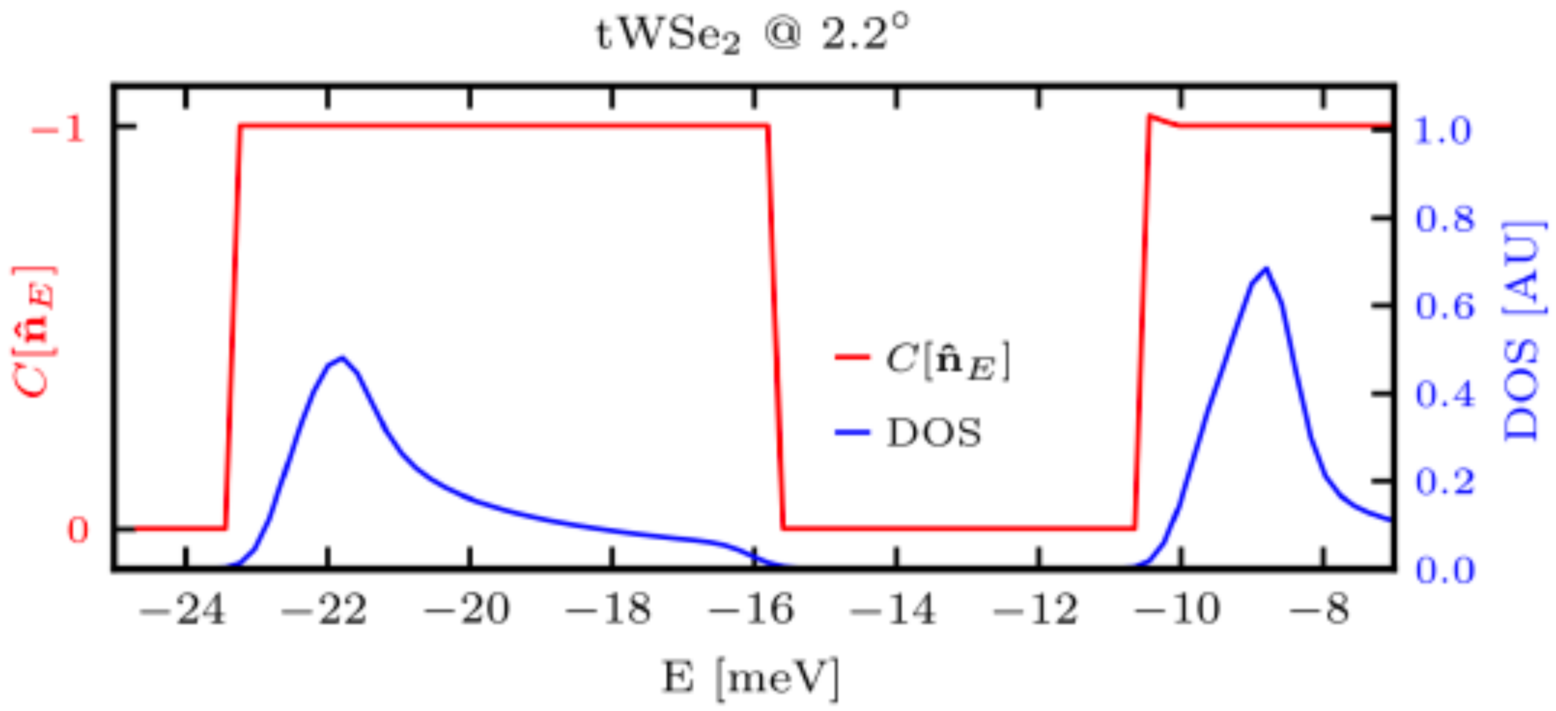

The real-space Chern number extracted from the ensemble average is consistently -1 - for the topmost two bands with (momentum) Chern number +1

Ensemble of WFs - TBG

Real-space Berry curvatures

Realistic corrugation $w_{AA}/w_{BA} = 0.7$

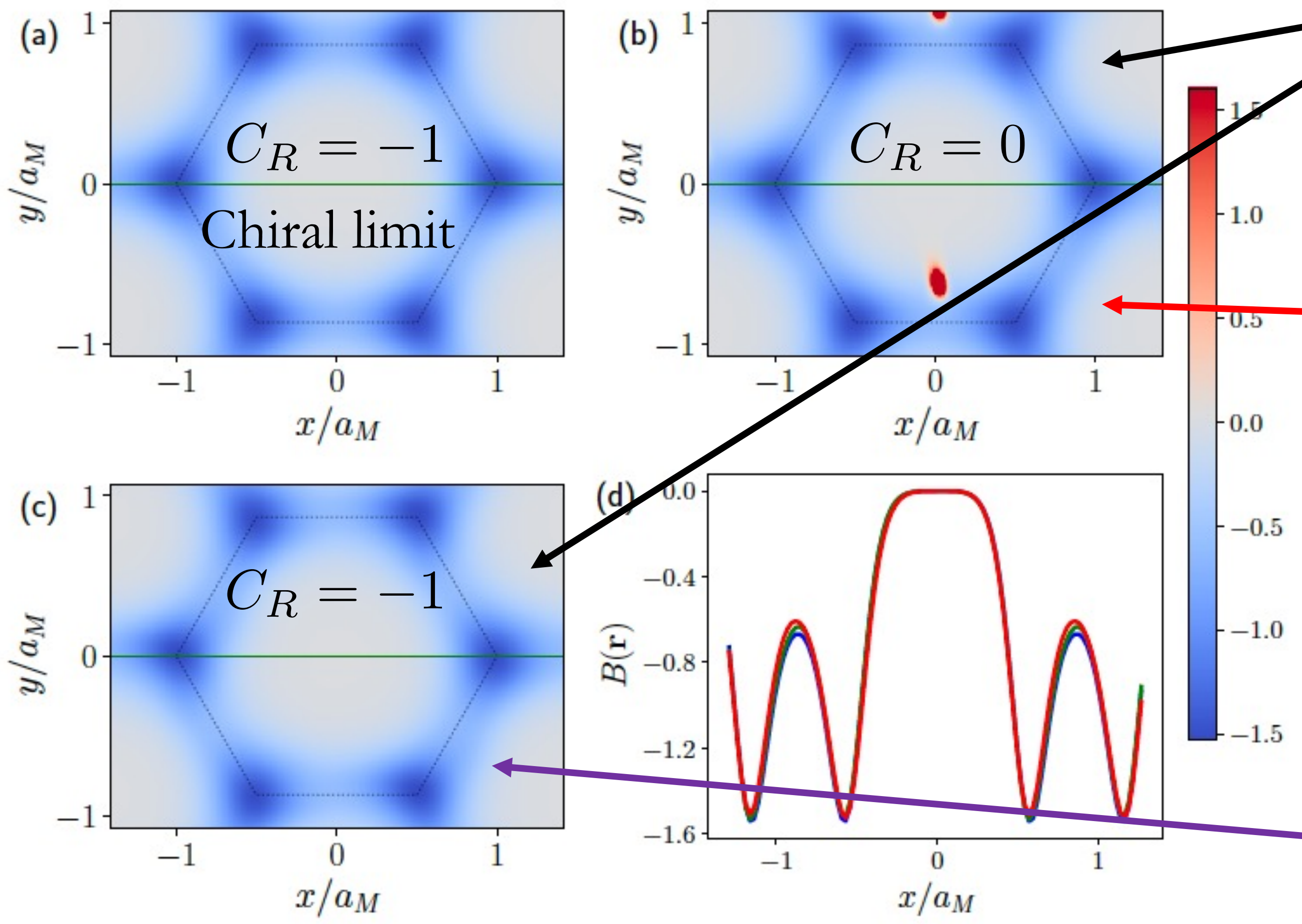

Individual WF at representative k

Ensemble of WF

Topological Heavy fermion model

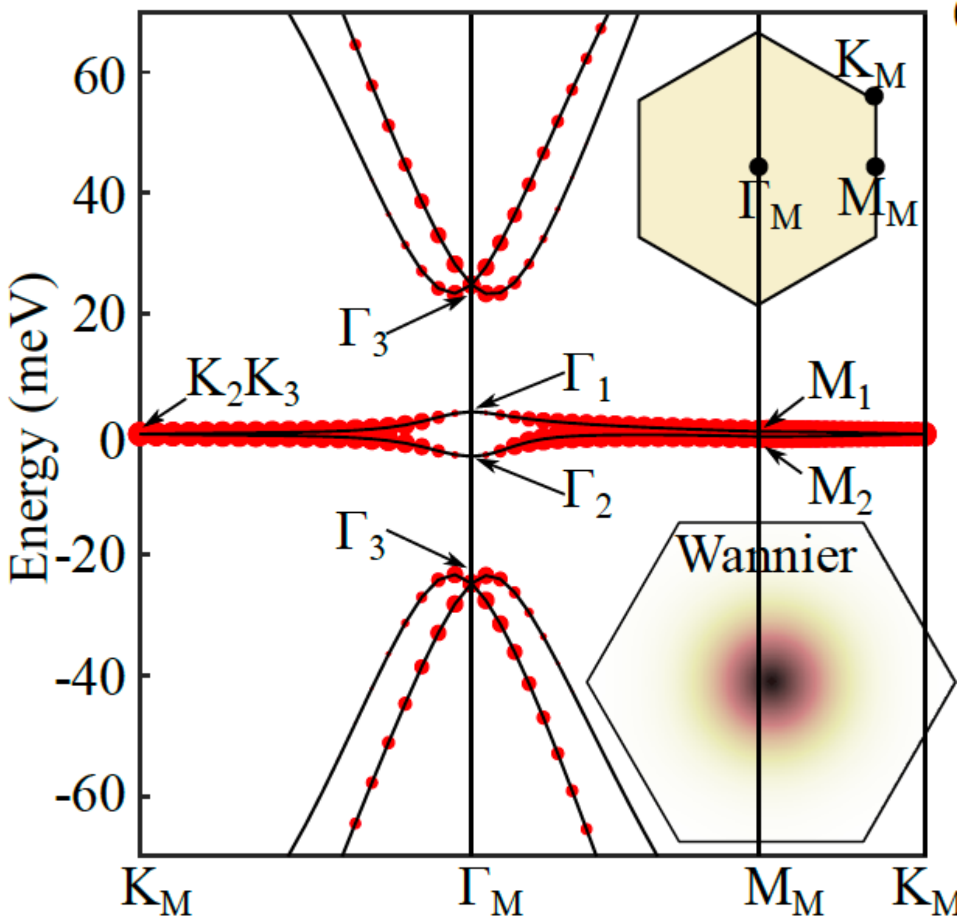

Six-band model reproduces the spectrum of TBG:

2 local Wannier orbitals (non-dispersive)

4 topological conduction bands

Successful in describing the coexistence of local moments and itinerants electrons

Song & Bernevig Phys Rev Lett 2022

Clugru Borovkov Lau Coleman Song & Bernevig, Low Temp Phys 2023

Shi & Dai Phys Rev B 2022

Real-space topology in the topological Heavy fermion model

Electronic distributions for the six different orbitals

Real-space Berry curvature for the six orbital WFs

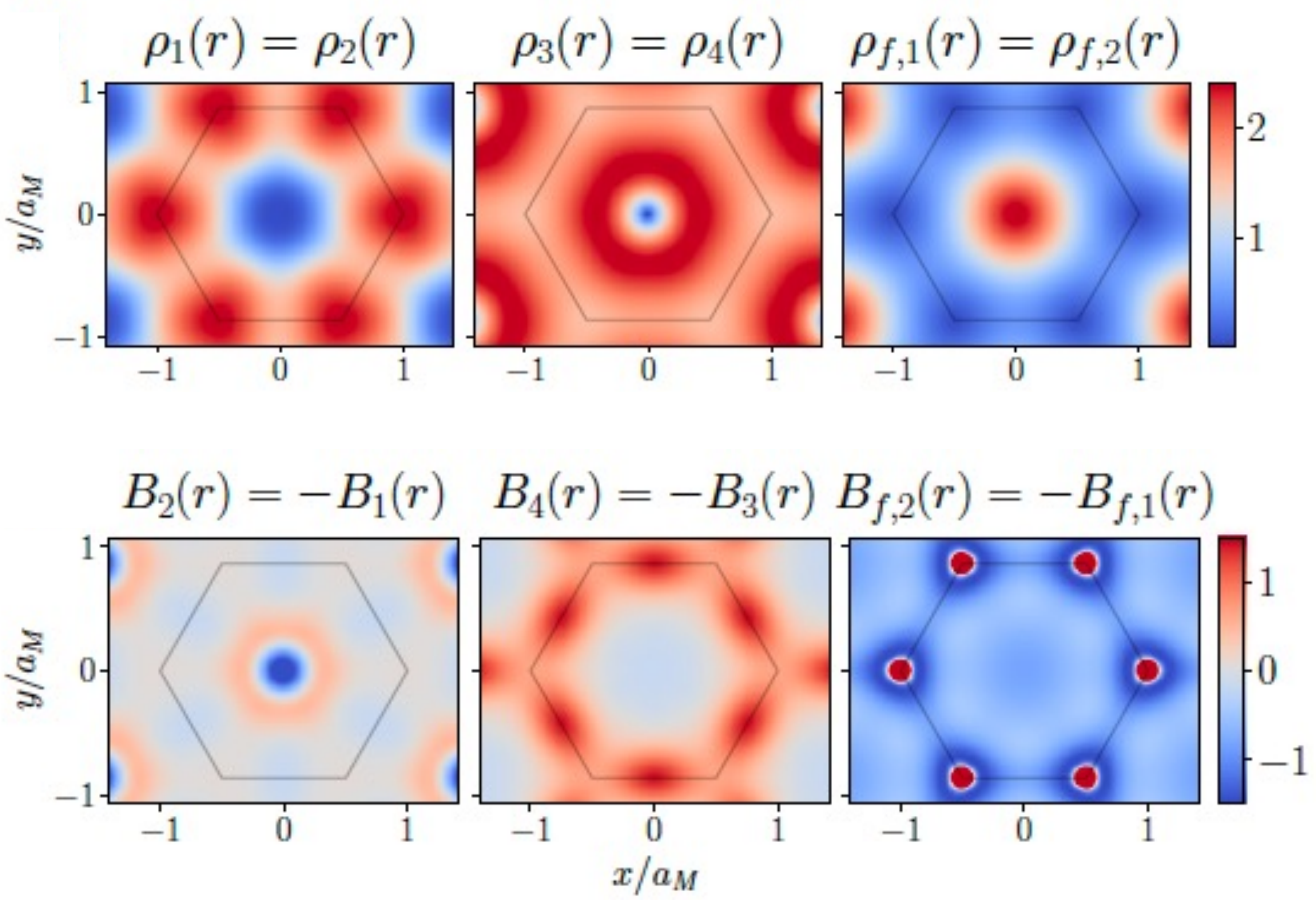

Real-space topology in the topological Heavy fermion model

Electronic distributions for the six different orbitals

Real-space Berry curvature for the six orbital WFs

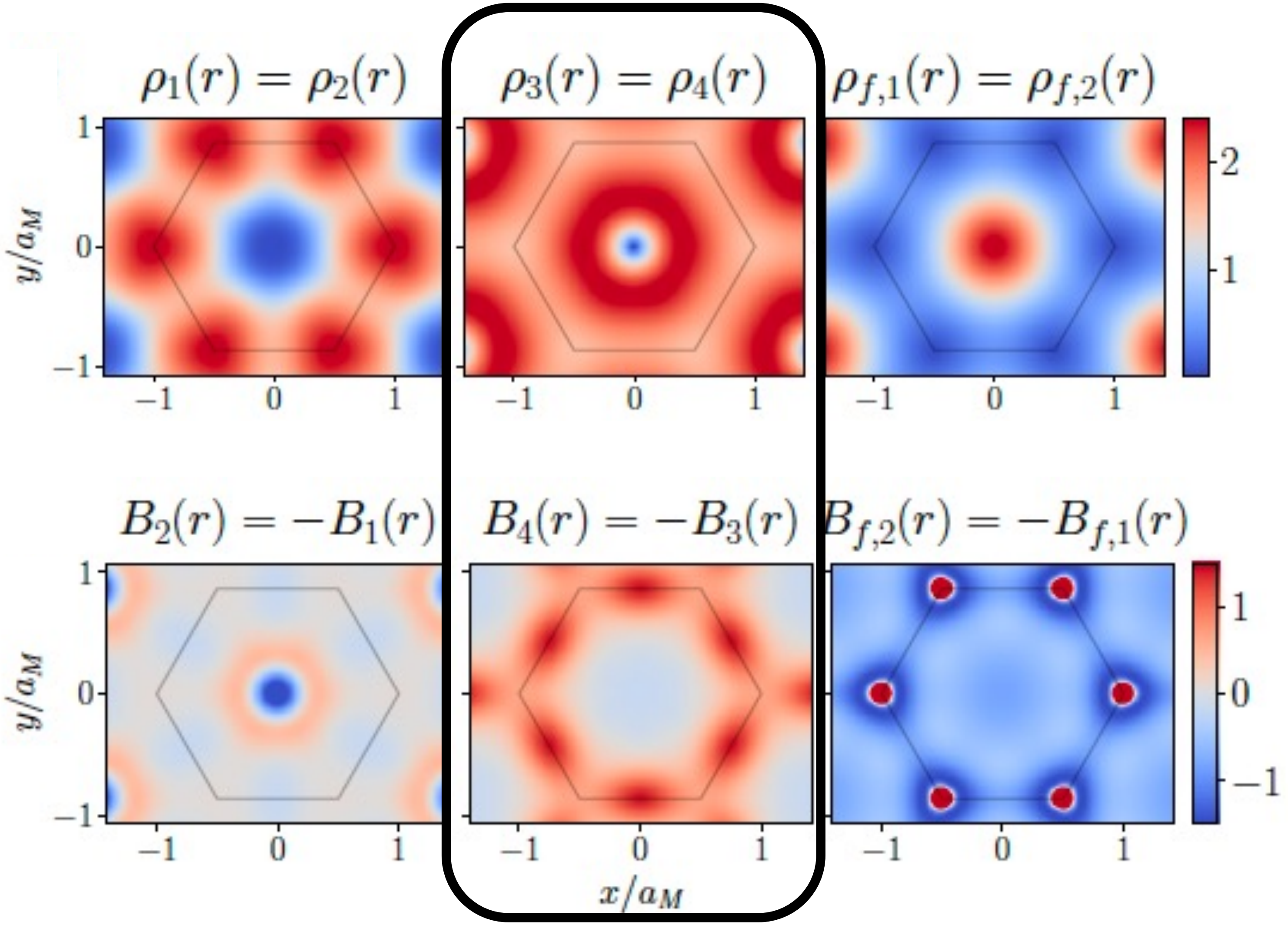

Symmetries for TMDs

In contrast with individual Bloch WFs (at fixed k), the ensemble-average inherits the (spatial) symmetries of the model

$$\boldsymbol{A}(E,\mathbf{r}) = \sum_{\mathbf{k}} u^\dagger_{\mathbf{k}}(\mathbf{r})\boldsymbol{\sigma} u_{\mathbf{k}}(\mathbf{r})\delta(\epsilon_{\mathbf{k}} - E)$$

$$\hat{\boldsymbol{n}}_E(\mathbf{r}) = \frac{\boldsymbol{A}(E,\mathbf{r})}{|\boldsymbol{A}(E,\mathbf{r})|}$$

Example of TMDs : two symmetries C_{3z} and $C_{2y}T$ – assuming valley polarization

$$\hat{\boldsymbol{n}}_E(C_{3z}\mathbf{r}) = R_z(\mathbf{b}_1 \cdot \mathbf{r})\hat{\boldsymbol{n}}_E(\mathbf{r})$$

$$\hat{\boldsymbol{n}}_E(C_{2y}\mathbf{r}) = M_z\hat{\boldsymbol{n}}_E(\mathbf{r})$$

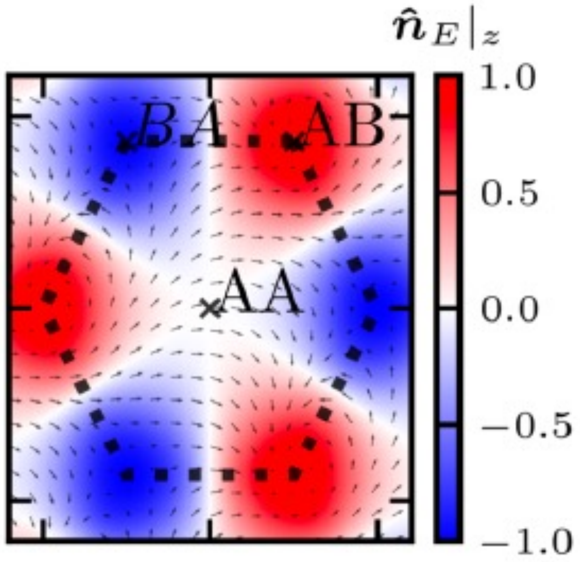

$$\hat{\boldsymbol{n}}_E(AA)|_z = 0$$

$$\hat{\boldsymbol{n}}_E(AB) = (0,0,\pm 1)$$

$$\hat{\boldsymbol{n}}_E(BA) = (0,0,\mp 1)$$

Symmetry indicators for real-space topology

$$\boldsymbol{A}(E,\mathbf{r}) = \sum_{\mathbf{k}} u_{\mathbf{k}}^\dagger(\mathbf{r})\boldsymbol{\sigma} u_{\mathbf{k}}(\mathbf{r})\delta(\epsilon_{\mathbf{k}} - E)$$

$$\hat{\boldsymbol{n}}_E(\mathbf{r}) = \frac{\boldsymbol{A}(E,\mathbf{r})}{|\boldsymbol{A}(E,\mathbf{r})|}$$

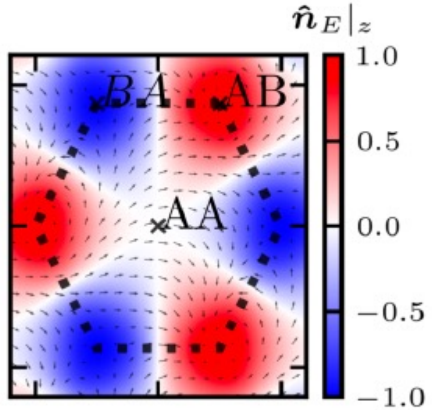

$$\hat{\boldsymbol{n}}_E(AA)|_z = 0$$
$$\hat{\boldsymbol{n}}_E(AB) = (0,0,\pm 1)$$
$$\hat{\boldsymbol{n}}_E(BA) = (0,0,\mp 1)$$

Symmetry indicators relate the Chern number to the C_{3z} eigenvalues at high-symmetry positions

$$e^{i2\pi C[\hat{\boldsymbol{n}}_E]/3} = \theta(AA)\theta(AB)\theta(BA) = \pm 1 \mod 3$$

For twisted TMDs, the real-space Chern number is always non-trivial !

Same non-trivial real-space Chern number in TBG

Same symmetries, C_{3z} and $C_{2y}T$ apply in TBG – assuming valley and sublattice polarization

The resulting real-space Chern number is therefore also always non-trivial

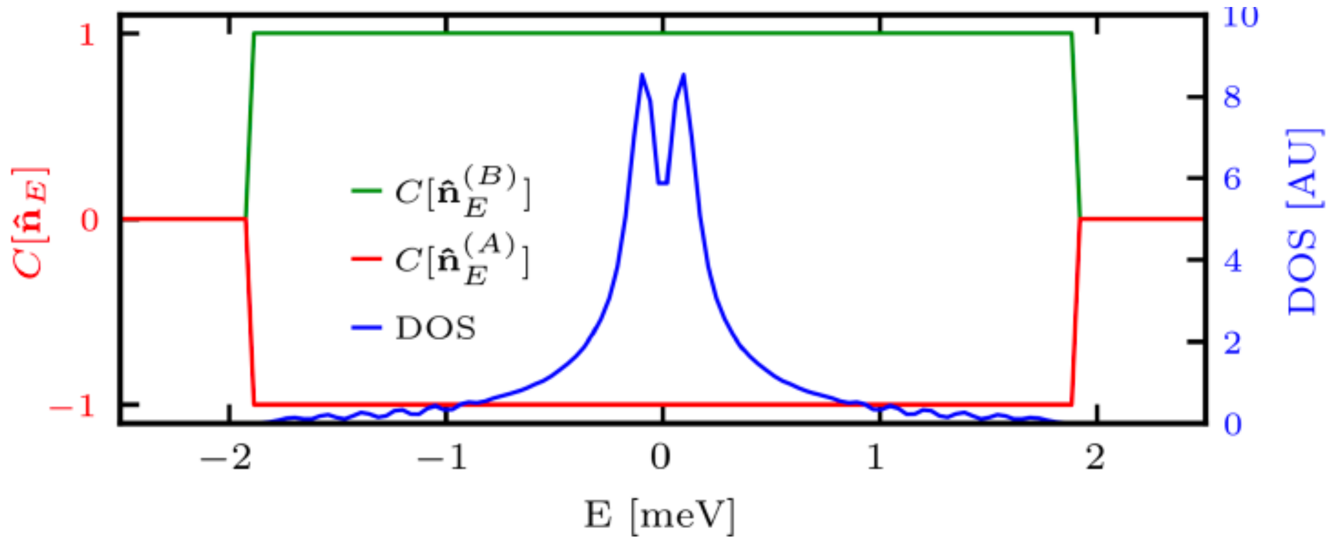

Experiments on layer-skyrmions textures

WSe_2

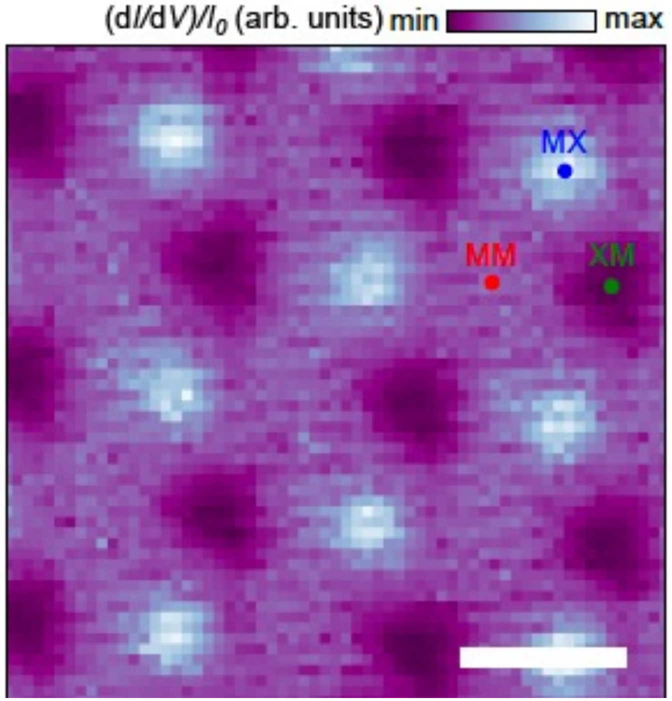

Zhang, Morales-Durán, Li, Yao, Su, Lin, Dong, Liu, Chen, Kim, Watanabe, Taniguchi, Li, Robinson, MacDonald & Shih. Nature Physics, 2024

$MoTe_2$

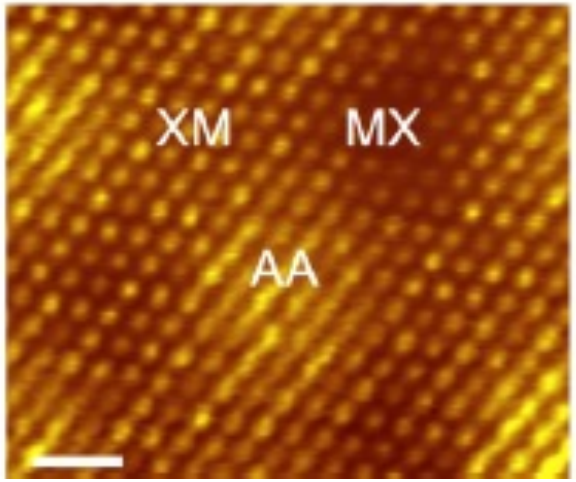

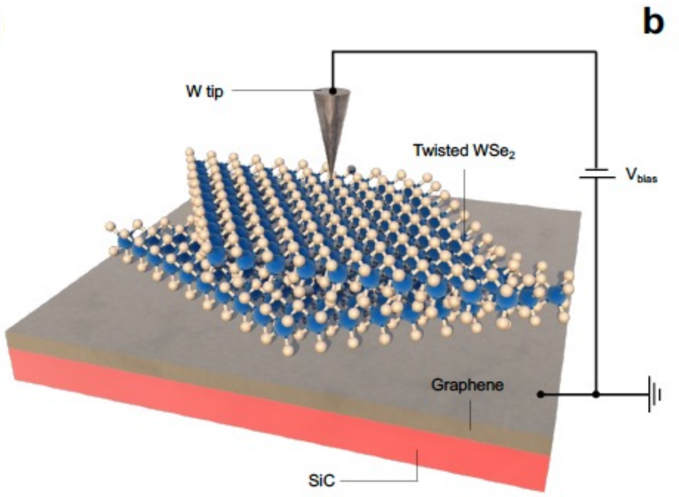

Thompson, Chu, Mesple, Zhang, Hu, Zhao, Park, Cai, Anderson, Watanabe, Taniguchi, Yang, Chu, Xu, Cao, Xiao & Yankowitz. Nature Physics, 2024.

Acknowledgments

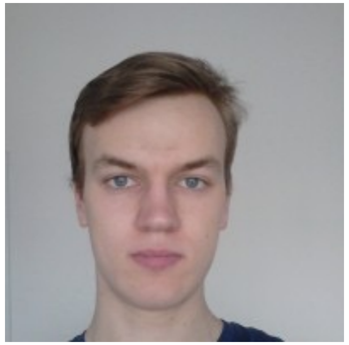

Kryštof Kolář

Felix von Oppen

Kang Yang

Daniele Guerci

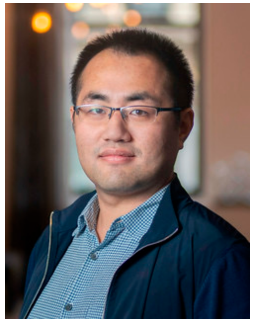

Jie Wang

Conclusion

Kolar, K. Wang, von Oppen, Mora PRB 2024
Guerci J. Wang, Mora Arxiv 2408.12652
Kolar, K. Wang, von Oppen, Mora, in preparation

Decomposition of the WF into a LL and a spinor with a layer-skyrmion texture in twisted TMDs in the adiabatic limit and chiral TBG

Non-trivial real-space Chern number associated with the skyrmion

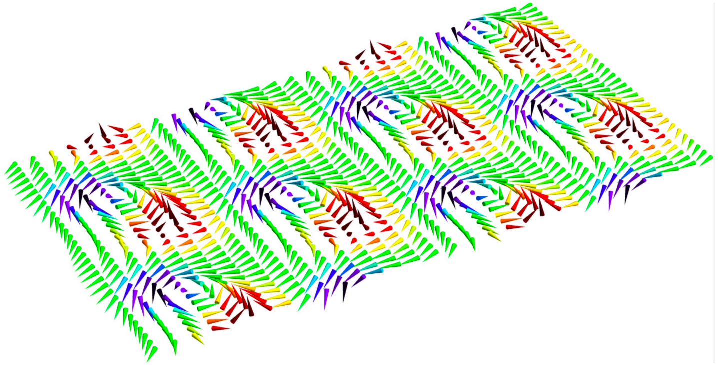

Fragile outside the adiabatic and chiral limits : Chern is zero

Ensemble of wavefunctions: defines a robust real-space Chern number.
Always non-zero in TMDs and TBG because of spatial symmetries

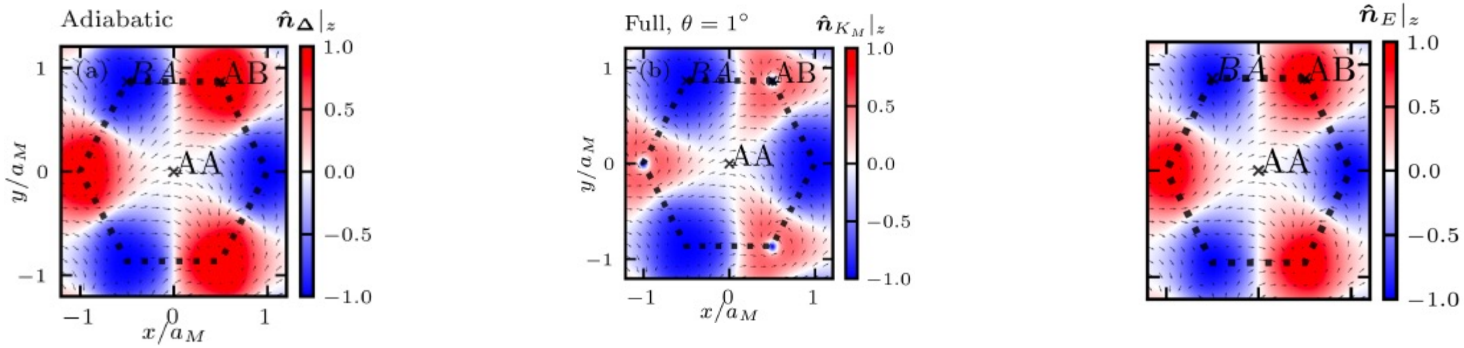

Adiabatic approximation

Morales-Durán, Wei, Shi, and MacDonald, 2024. Phys. Rev. Lett. 132, 096602.

Zhai and Yao, 2020. Phys. Rev. Mater. 4, 094002.

Bruno, Dugaev, and Taillefumier, 2004. Phys. Rev. Lett. 93, 096806.

$tMoTe_2$

E. Thompson, K. T. Chu, F. Mesple, X.-W. Zhang, …., X. Xu, T. Cao, D. Xiao, and M. Yankowitz, Arxiv 2024

$tWSe_2$

F. Zhang, N. Morales-Duran,…, J. A. Robinson, A. H. Macdonald, and C.-K. Shih, Arxiv 2024

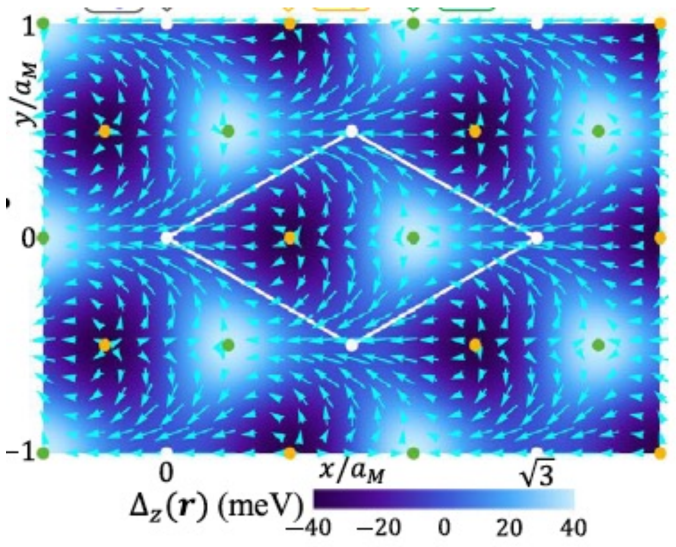

Full Pontryagin index = integrated flux = 1 !

Pontryagin density (or Berry phase) of a skyrmion texture

$$\hat{n}(\mathbf{r}) = \frac{\boldsymbol{\Delta}(\mathbf{r})}{|\boldsymbol{\Delta}(\mathbf{r})|} \qquad \tilde{B}(\mathbf{r}) = -\frac{\hbar}{2e}\hat{\mathbf{n}}(\mathbf{r}) \cdot \partial_x \hat{\mathbf{n}}(\mathbf{r}) \times \partial_y \hat{\mathbf{n}}(\mathbf{r})$$

Layer skyrmions in twisted bilayer graphene

Layer skyrmions for ideal Chern bands and twisted bilayer graphene

Daniele Guerci,[1] Jie Wang,[2] and Christophe Mora[3]

[1] *Center for Computational Quantum Physics, Flatiron Institute, New York, New York 10010, USA*
[2] *Department of Physics, Temple University, Philadelphia, Pennsylvania, 19122, USA*
[3] *Université Paris Cité, CNRS, Laboratoire Matériaux et Phénomènes Quantiques, 75013 Paris, France*

arXiv:2408.12652v1

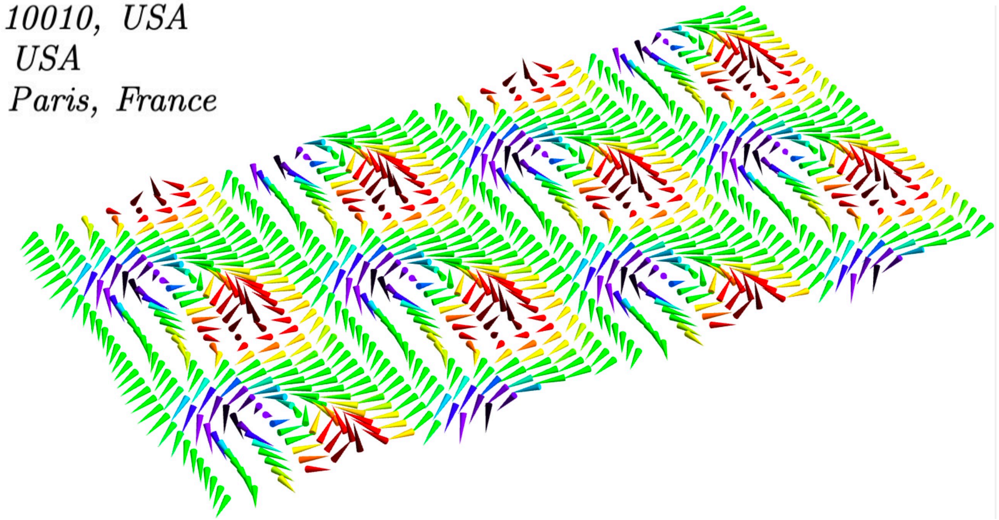

Magnetic boundary condition

Ledwith, Tarnopolsky, Khalaf, Vishwanath, PRR 2020
Wang, Cano, Millis, Liu, Yang, PRL 2021

Twisted TMDs

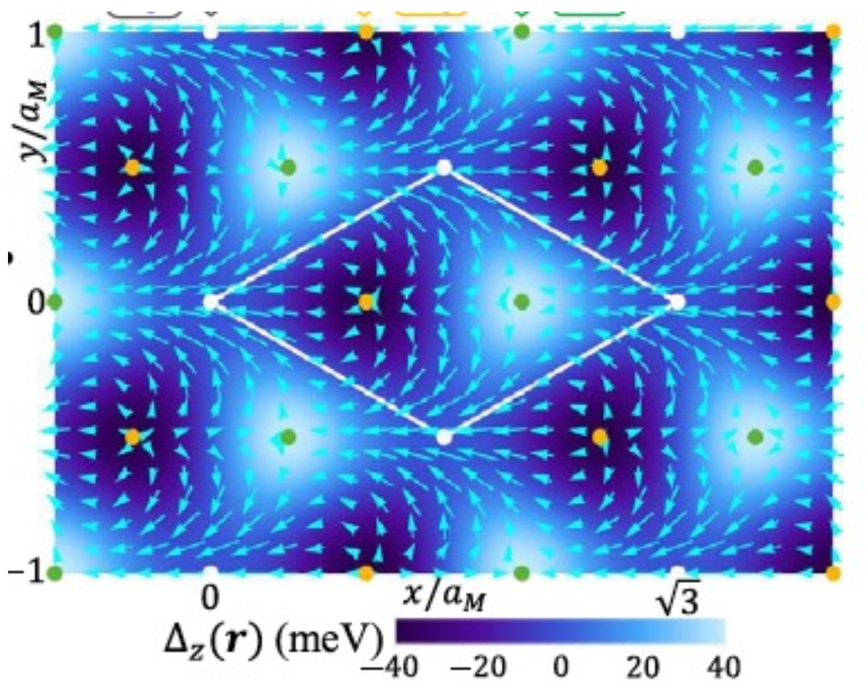

Twisted bilayer graphene (chiral)

$$\psi_{\boldsymbol{k}}(\boldsymbol{r}) = \chi(\boldsymbol{r})\,\Phi^{LLL}_{\boldsymbol{k}}(\boldsymbol{r})$$

Bloch BC

Magnetic translation BC

Berry phase of the spinor (under winding) **screens** the magnetic phase

$$\chi(\boldsymbol{r}+\boldsymbol{a}_j) = e^{-i(\boldsymbol{a}_j\times\boldsymbol{r})/2l_B^2}\,\chi(\boldsymbol{r})$$

Skyrmions texture for the layer index

Twisted bilayer graphene (chiral)

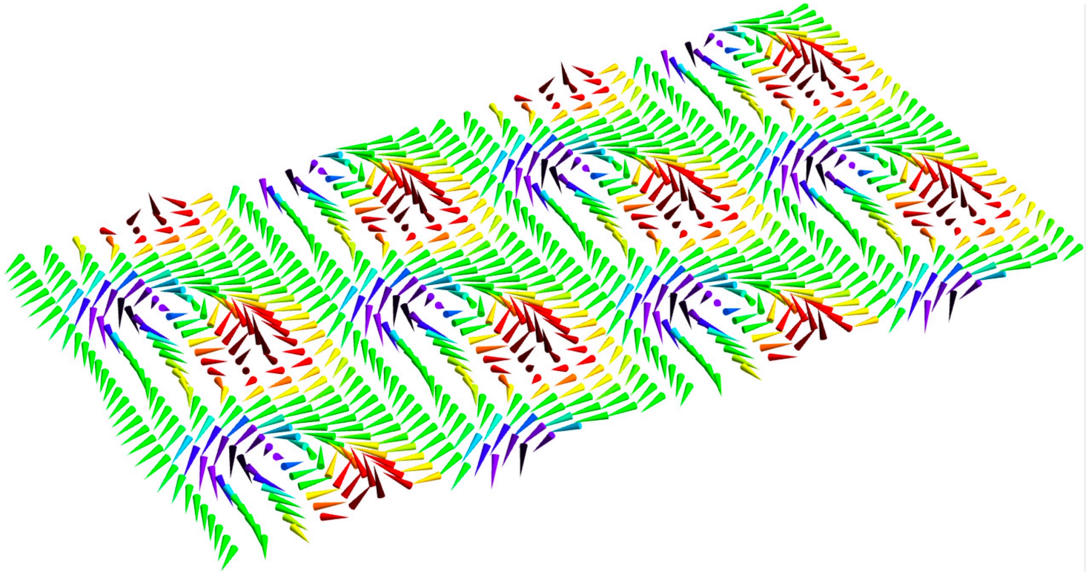

Triangular Skyrme texture in the layer index

Realistic twisted bilayer graphene (non-chiral)

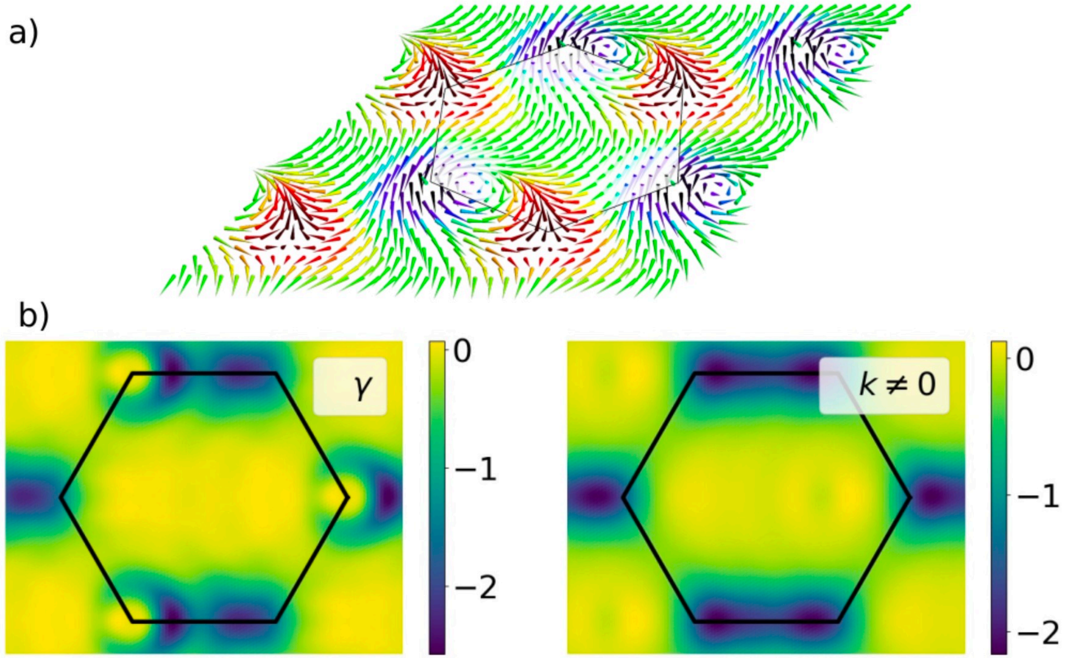

Fractional Chern insulators in $MoTe_2$

Twist angle around $\theta = 3.7^\circ$

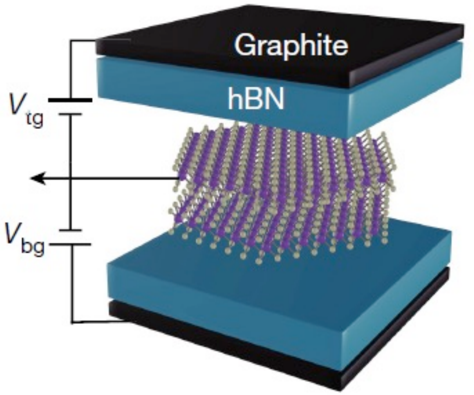

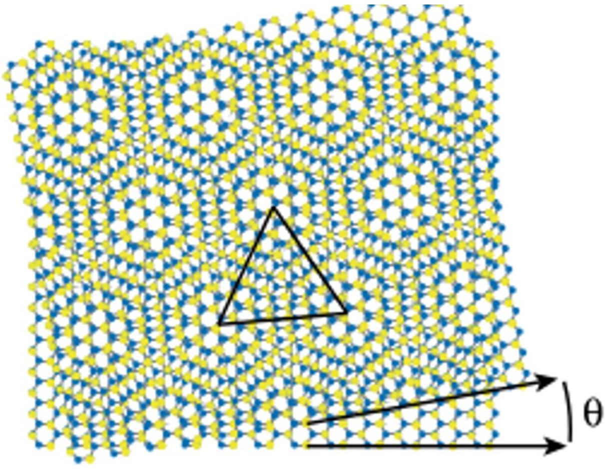

Optical evidence

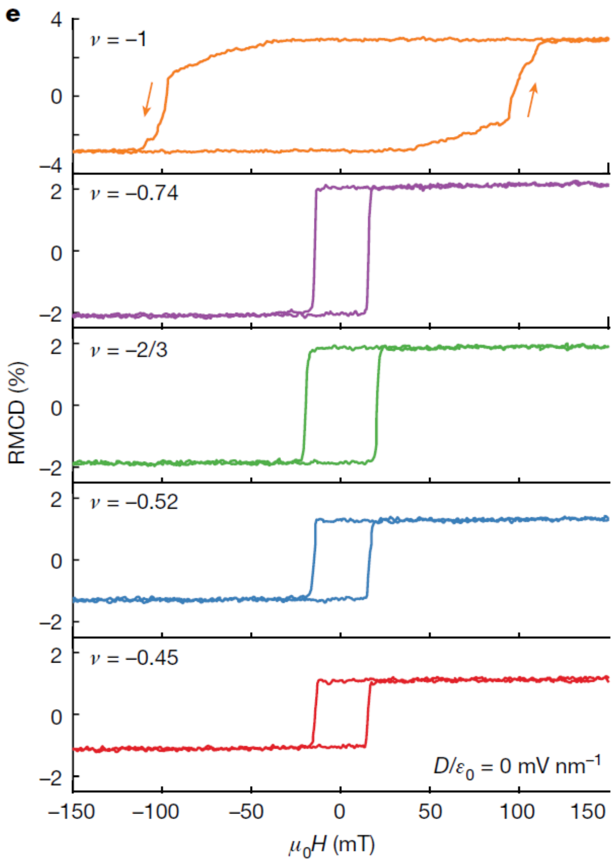

Cai, Anderson, Wang, Zhang, Liu, Holtzmann, Zhang, Fan, Taniguchi, Watanabe, Ran, Cao, Fu, Xiao, Yao, and Xu, Nature 2023

Capacitance (compressibility)

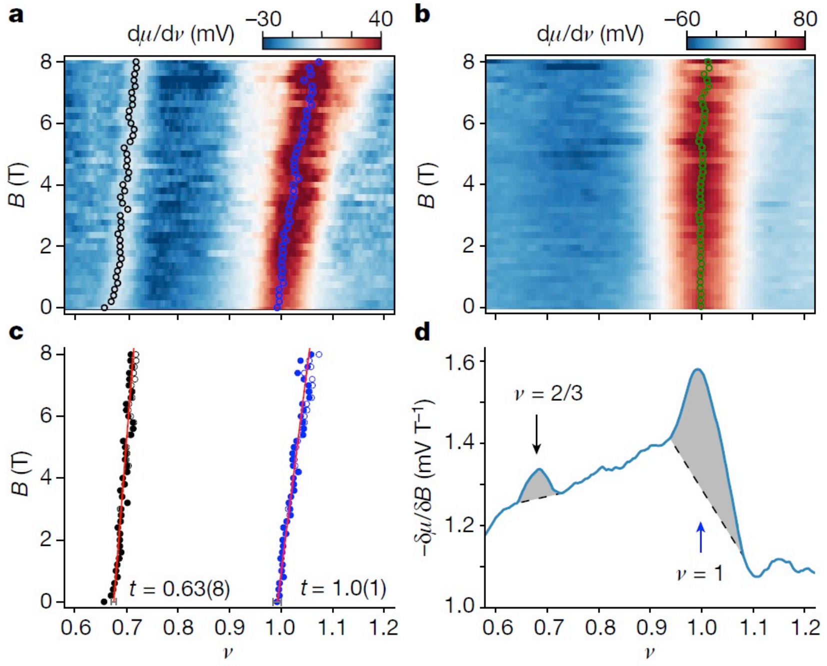

Zeng, Xia, Kang, Zhu, Knüppel, Vaswani, Watanabe, Taniguchi, Mak, and Shan, 2023. Nature 622, 69–73.

Continuum model in a magnetic field

Herzog-Arbeitman, Chew, Bernevig PRB 2022

$$H_{\rm sp}^K = \begin{pmatrix} -\frac{\hbar^2(\mathbf{k}-\mathbf{K}^b)^2}{2m^*} + V_b(\mathbf{r}) & T(\mathbf{r}) \\ T^\dagger(\mathbf{r}) & -\frac{\hbar^2(\mathbf{k}-\mathbf{K}^t)^2}{2m^*} + V_t(\mathbf{r}) \end{pmatrix}$$

Minimal coupling $\quad \mathbf{k} \to \mathbf{\Pi} = \mathbf{k} - e\mathbf{A}/\hbar$

$$(\Pi_x^2 + \Pi_y^2)\,|n,\mathbf{k}\rangle = (n+\frac{1}{2})\frac{1}{l_B^2}\,|n,\mathbf{k}\rangle$$

$$T_{q\mathbf{a}_1}\,|n,\mathbf{k}\rangle = e^{iq\mathbf{a}_1\cdot\mathbf{k}}\,|n,\mathbf{k}\rangle$$

$$T_{\mathbf{a}_2/p}\,|n,\mathbf{k}\rangle = e^{i\frac{1}{p}\mathbf{a}_2\cdot\mathbf{k}}\,|n,\mathbf{k}\rangle$$

Gauge invariant method

Commensurate flux $\quad \frac{\Phi}{\Phi_0} = \frac{p}{q}$

Set of commutating operators:
kinetic energy and magnetic translations

$\mathbf{\Pi} \qquad T_{q\mathbf{a}_1} \qquad T_{\mathbf{a}_2/p}$

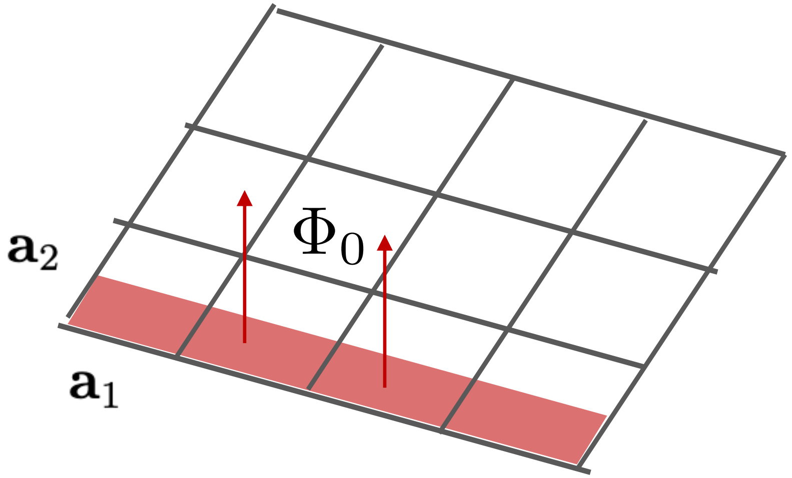

Bloch Landau levels

Implicit solution, eigenstate of $\mathbf{\Pi}, T_{q\mathbf{a}_1}, T_{\mathbf{a}_2/p}$

$$\boxed{|n, \mathbf{k}\rangle = e^{i\mathbf{k}\cdot\mathbf{R}}\, |n, 0\rangle}$$

guiding center

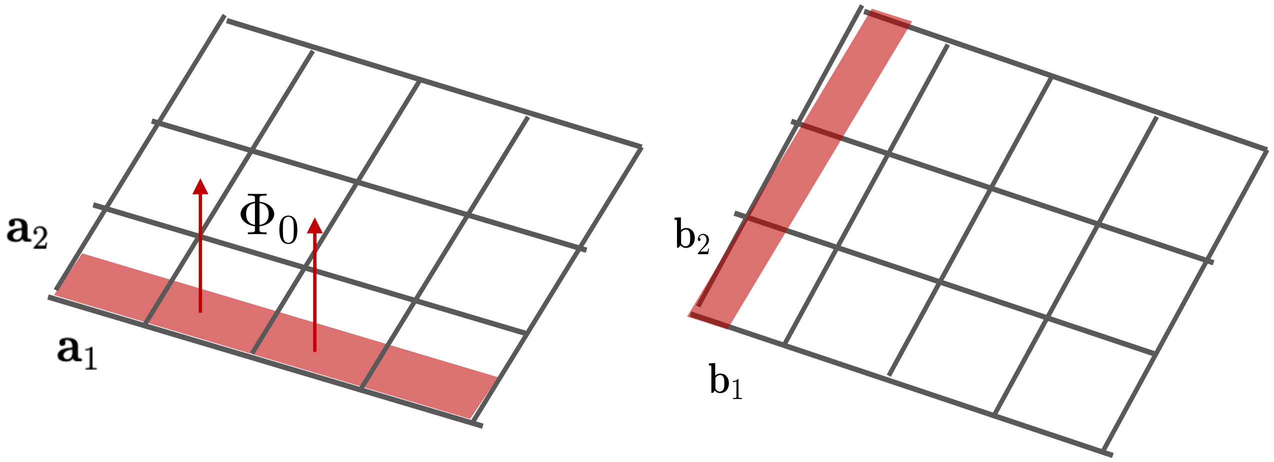

$$\langle \mathbf{k}', n'| e^{i(m_1\mathbf{b}_1 + m_2\mathbf{b}_2)\cdot\mathbf{r}} |n, \mathbf{k}\rangle = \delta_{\mathbf{k}',\mathbf{k}+m_2\mathbf{b}_2} \exp\left(-i\pi m_1 m_2 \frac{q}{p}\right)$$

$$\exp(-i2\pi k_1 \lfloor k_2 + m_2/p \rfloor) \exp\left\{ i2\pi(k_2 p + m_2)\frac{q}{p} m_1 \right\}$$

$$\times (z^*)^{n'-n} \sqrt{\frac{n'!}{n!}} L_{n'}^{n-n'}(|z|^2) \exp(-|z|^2/2)$$

$$z = (m_1 b_1 + m_2 b_2)\frac{\ell_B}{\sqrt{2}}$$

Explicit form of the Bloch LL is not needed. Gauge invariant construction.

(Fractional) Chern insulator in $MoTe_2$

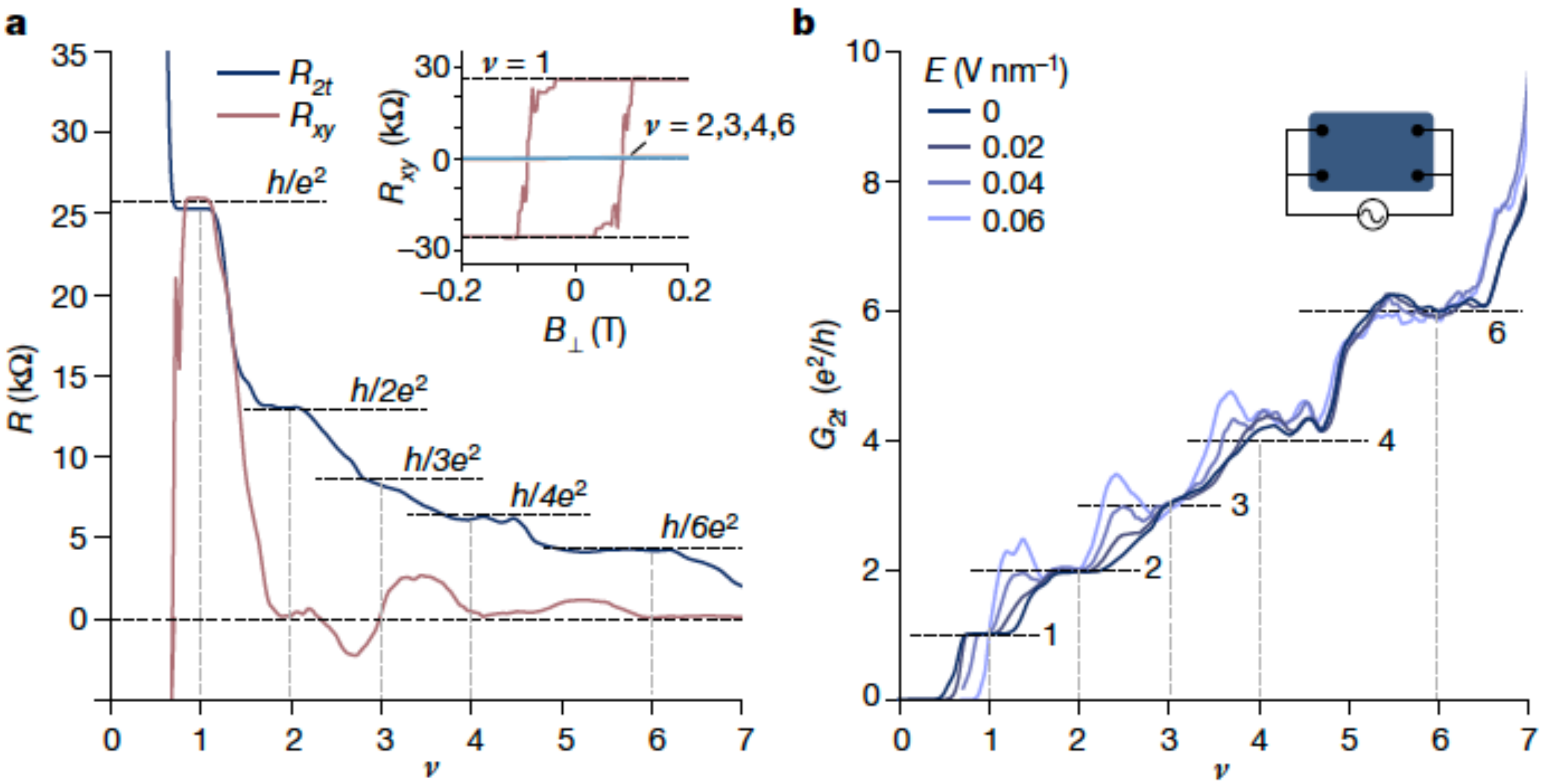

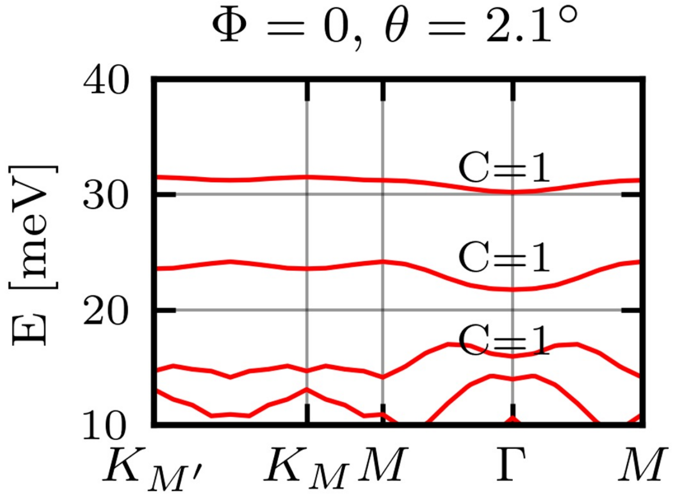

Kang, Shen, Qiu, Zeng, Xia,
Watanabe, Taniguchi, Shan, and
Mak, 2024. Nature 628, 522–526.

Streda formula

$\theta = 1^\circ$